

Newly High-T_g Bipolar Benzimidazole Derivatives in Improving Stability of High-Efficiency OLEDs

Sheng-Jie Lin,^a Yu-Chieh Cheng,^b Chia-Hsun Chen,^{a,b} Yong Yun Zhang,^b Jiun-Haw Lee,^{*a}
Man-kit Leung,^{*b} Bo-Yen Lin,^{*c} and Tien-Lung Chiu^{*d}

^aGraduate Institute of Photonics and Optoelectronics and Department of Electrical Engineering,
National Taiwan University, Taipei 10617, Taiwan.

^bDepartment of Chemistry, National Taiwan University, Taipei 10617, Taiwan.

^cDepartment of Opto-Electronic Engineering, National Dong Hwa University, Hualien 974301, Taiwan.

^dDepartment of Electrical Engineering, Yuan Ze University, Taoyuan 32003, Taiwan.

*Email: jiunhawlee@ntu.edu.tw (J.-H. Lee); mkleung@ntu.edu.tw (M.k. Leung); boyenlin@gms.ndhu.edu.tw (B.-Y. Lin); tlchiu@saturn.yzu.edu.tw (T.-L. Chiu)

Table of Contents

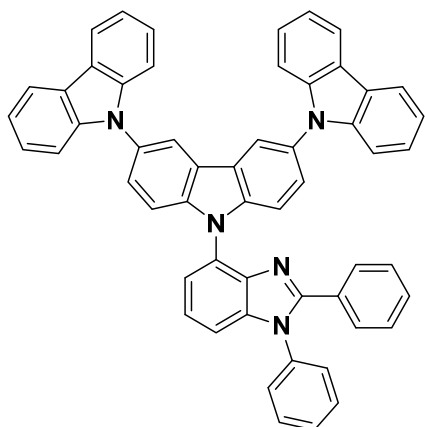
General synthetic procedure for 1 , 2 , 3 , and 4-3cbzBIZ 's	S3-S7
Fig. S1. ¹ H NMR spectrum of 5	S8
Fig. S2. ¹³ C NMR spectrum of 5	S9
Fig. S3. ¹ H NMR spectrum of 4-3cbzBIZ	S10
Fig. S4. ¹³ C NMR spectrum of 4-3cbzBIZ	S11
Fig. S5. ¹ H NMR spectrum of 3-3cbzBIZ	S12
Fig. S6. ¹³ C NMR spectrum of 3-3cbzBIZ	S13
Fig. S7. ¹ H NMR spectrum of 2-3cbzBIZ	S14
Fig. S8. ¹³ C NMR spectrum of 2-3cbzBIZ	S15
Fig. S9. ¹ H NMR spectrum of 1-3cbzBIZ	S16
Fig. S10. ¹³ C NMR spectrum of 1-3cbzBIZ	S17
Fig. S11. ORTEP of 1-3cbzBIZ	S18
Fig. S12. ORTEP of 2-3cbzBIZ	S20
Fig. S13. ORTEP of 3-3cbzBIZ	S22
Fig. S14. ORTEP of 4-3cbzBIZ	S24
Fig. S15. Thermogravimetric analysis of 3cbzBIZ 's	S26
Fig. S16. Differential scanning calorimetric analysis of 3cbzBIZ 's	S27
Fig. S17. Spectrometric analysis of 3cbzBIZ 's, including UV-Vis, room temperature steady-state fluorescence, and low temperature fluorescence and phosphorescence spectral data at 77K.	S28

Fig. S18 Photoelectron spectra of 1 -, 2 -, and 4-3cbzBIZ from AC2 measurements.	S30
Fig. S19 Photoluminescence spectra of 1 -, 2 -, and 4-3cbzBIZ and the absorption spectrum of FIrpic .	S31
Fig. S20 Device performance of (a) J-V; (b)CE-J; (c)PE-J; (d) EQE-J for device B-1 to B-5 using 1-3cbzBIZ as host.	S32
Fig. S21 Device performance of (a) J-V; (b)CE-J; (c)PE-J; (d) EQE-J for devices C-1 to C-5 using 2-3cbzBIZ as host	S33
Fig. S22 Device performance of (a) J-V; (b)CE-J; (c)PE-J; (d) EQE-J for device C-1 to C-5 using 4-3cbzBIZ as host.	S34
Fig. S23 Luminance decay curves for 4-3cbzBIZ, 2-3cbzBIZ and 1-3cbzBIZ in blue OLEDs at initial luminance of 1000 cd/m ² .	S35
Fig. S24 Driving voltage changes with aging time for initial luminescence of (a) 10000; (b) 20000; (c) 30000 cd/m ²	S35
Fig. S25 Luminance decay curves of (a) 4-3cbzBIZ and (b) CBP devices under different temperature at initial luminance of 10000 cd/m ² .	S35
Fig. S26 PL spectra of doped films of (a) 4-3cbzBIZ :10%Ir(ppy) ₃ and (b) CBP: 10%Ir(ppy) ₃ before and after with annealing of 40 °C, 60 °C, 80 °C for 30 mins.	S36
Fig. S27 AFM images of doped films before and after annealing at a high temperature (80 °C) of 4-3cbzBIZ :10%Ir(ppy) ₃ (a) before (b) after, and CBP: 10%Ir(ppy) ₃ (c) before (d) after, respectively.	S36
Table S1 Crystal data and experimental details for 1-3cbzBIZ	S19
Table S2 Crystal data and experimental details for 2-3cbzBIZ	S21
Table S3 Crystal data and experimental details for 3-3cbzBIZ	S23
Table S4 Crystal data and experimental details for 4-3cbzBIZ	S25
Table S5. The theoretical HOMO and LUMO information of 3cbzBIZ 's in THF was predicted by the Ab initio calculation method at BLYP-D3/6-311+G(d) level.	S29
Table S6 Device structure of device B-1 to B-5.	S32
Table S7 Device performance for device B-1 to B-5.	S32
Table S8 Device structure of devices C-1 to C-5.	S33
Table S9 Device performance for devices C-1 to C-5.	S33
Table S10 Device structure of devices D-1 to D-7.	S34
Table S11 Device performance for devices D-1 to D-7.	S34

The starting materials **1-4** were prepared according to the procedures reported in ref. 10 in the manuscript.

General synthetic procedure for **2**, **3**, and **4-3cbzBIZ**'s

9-(1,2-Diphenyl-1*H*-benzo[*d*]imidazol-4-yl)-9*H*-3,6-di(*N*-carbazolyl)carbazole (**4-3cbzBIZ**)



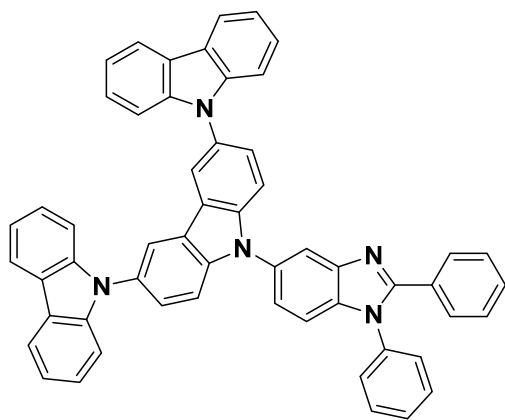
4-3cbzBIZ

To a mixture of 4-bromo-1,2-diphenyl-1*H*-benzimidazole (**1**) (0.73 g, 2.1 mmol), 9*H*-3,6-di(*N*-carbazolyl)carbazole (**Tcbz**) (1.09 g, 2.2 mmol), copper (I) iodide (CuI, 0.016 g, 0.08 mmol), potassium carbonate (K₂CO₃, 0.87 g, 6.3 mmol) was added dimethylacetamide (DMAc, 2.1 mL). The mixture was reacted at 180 °C for 16 h. After completion of the reaction, DMAc was removed by distillation under vacuum. The residue was taken up with chloroform. The insoluble salt was removed by filtration through celite. The filtrate was washed with brine. The organic extracts were dried over anhydrous magnesium sulfate and concentrated by rotary evaporation to give crude residue that was further purified by liquid chromatography on silica gel, using hexanes/dichloromethane (1:2) as the eluent to give **4-3cbzBIZ** as colourless crystals (1.2 g, 75% yield).

¹H NMR (400 MHz, CD₂Cl₂): δ 8.36 (s, 2H), 8.17 (d, *J* = 7.8 Hz, 4H), 7.72-7.67 (m, 3H), 7.64-7.54 (m, 8H), 7.50-7.45 (m, 7H), 7.44-7.39 (m, 4H), 7.37-7.35 (m, 1H), 7.31-7.26 (m, 6H); ¹³C NMR (100

MHz, CD₂Cl₂): δ 153.68, 142.29, 141.73, 140.16, 140.03, 137.23, 130.59, 130.49, 130.17, 130.08, 129.44, 128.72, 128.23, 127.99, 126.35, 126.31, 124.57, 124.22, 123.49, 122.16, 120.55, 120.03, 119.97, 112.84, 111.40, 110.27. HRMS (ESI) m/z calcd for C₅₅H₃₆N₅ 766.2971, obsd. 766.3002 (M⁺). Anal. Calcd for C₅₅H₃₅N₅: C, 86.25; H, 4.61; N, 9.14; Found: C, 85.91; H, 4.54; N, 9.15.

9-(1,2-Diphenyl-1*H*-benzo[*d*]imidazol-5-yl)-9*H*-3,6-di(*N*-carbazolyl)carbazole (3-3cbzBIZ**)**

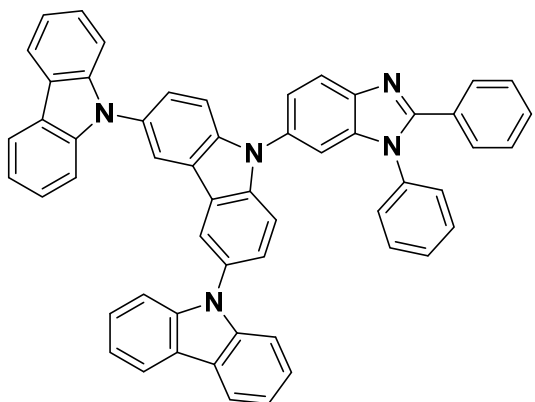


3-3cbzBIZ

3-Bromo-1,2-diphenyl-1*H*-benzimidazole (**2**) (0.61 g, 1.75 mmol), 9*H*-3,6-di(*N*-carbazolyl)carbazole (**Tcbz**) (0.91 g, 1.82 mmol), copper(I) iodide (CuI, 0.013 g, 0.07 mmol), potassium carbonate (0.72 g, 5.21 mmol) in dimethylacetamide (DMAc, 1.74 mL) were reacted to give crude product that was purified by liquid chromatography on silica gel, using hexanes/dichloromethane (1:3) as the eluent to give **3-3cbzBIZ** as colourless crystals (0.95 g, 71% yield).

¹H NMR (500 MHz, CD₂Cl₂): δ 8.33 (d, *J* = 2 Hz, 2H), 8.21 (d, *J* = 2 Hz, 1H), 8.17 (d, *J* = 7.5 Hz, 4H), 7.71 (d, *J* = 8.5 Hz, 2H), 7.75-7.68 (m, 8H), 7.55 (d, *J* = 8.5 Hz, 1H), 7.48-7.35 (m, 13H), 7.31-7.26 (m, 4H); ¹³C NMR (100 MHz, CDCl₃): δ 154.21, 141.97, 141.48, 137.07, 136.68, 132.53, 130.39, 130.33, 130.22, 129.67, 129.30, 128.68, 127.55, 126.41, 126.03, 123.95, 123.29, 123.05, 120.40, 119.86, 119.79, 118.93, 112.10, 111.50, 109.89. HRMS (ESI) m/z calcd for C₅₅H₃₆N₅ 766.2971, obsd. 766.2943 (M⁺). Anal. Calcd for C₅₅H₃₅N₅: C, 86.25; H, 4.61; N, 9.14; Found: C, 85.70; H, 4.49; N, 9.14.

9-(1,2-Diphenyl-1*H*-benzo[*d*]imidazol-6-yl)-9*H*-3,6-di(*N*-carbazolyl)carbazole (2-3cbzBIZ**)**



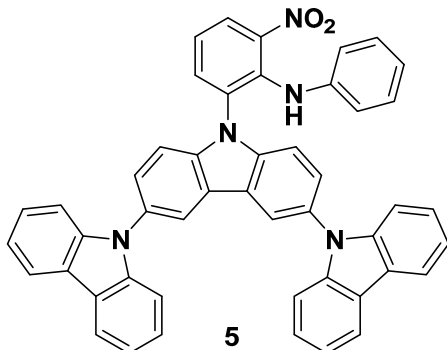
2-3cbzBIZ

2-Bromo-1,2-diphenyl-1*H*-benzimidazole (**3**) (0.58 g, 1.66 mmol), 9*H*-3,6-di(*N*-carbazolyl)carbazole (**Tcbz**) (0.87 g, 1.75 mmol), copper(I) iodide (CuI, 0.013 g, 0.07 mmol), potassium carbonate (0.69 g, 4.99 mmol) in dimethylacetamide (DMAc, 1.74 mL) were reacted to give crude product that was purified by liquid chromatography on silica gel, using hexanes/dichloromethane (1:5) as the eluent to give **2-3cbzBIZ** as colourless crystals (0.72 g, 57% yield).

¹H NMR (500 MHz, CD₂Cl₂): δ 8.29 (s, 2H), 8.16 (d, *J* = 7.5 Hz, 4H), 8.15 (d, *J* = 8.5 Hz, 1H), 7.69-7.58 (m, 8H), 7.56-7.48 (m, 3H), 7.46-7.35 (m, 13H), 7.30-7.25 (m, 4H); ¹³C NMR (100 MHz, CDCl₃): δ 154.11, 141.93, 141.45, 138.03, 136.37, 132.95, 130.45, 129.77, 129.44, 128.76, 127.46, 126.47, 126.02, 123.91, 123.39, 123.30, 121.31, 120.44, 119.88, 119.84, 111.37, 110.08, 109.82. HRMS (ESI) m/z calcd for C₅₅H₃₆N₅ 766.2971, obsd. 766.2948 (M⁺). Anal. Calcd for C₅₅H₃₅N₅: C, 86.25; H, 4.61; N, 9.14; Found: C, 85.86; H, 4.46; N, 9.13.

Preparation of 1-3cbzBIZ

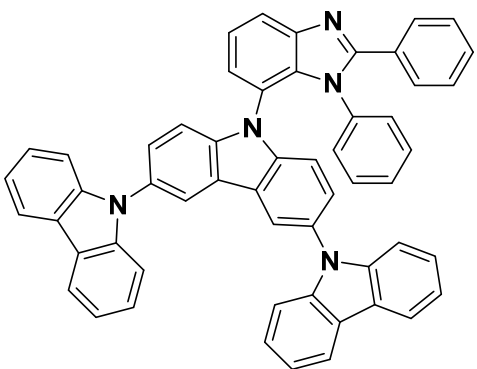
2-(9*H*-[3,6-Di(*N*-carbazolyl)carbazole]-9-yl)-6-nitro-N-phenylaniline (5**)**



A mixture of 2-fluoro-6-nitro-*N*-phenylbenzenamine (**4**) (0.35 g, 1.51 mmol), *9H*-3,6-di(*N*-carbazolyl)carbazole (**Tcbz**) (0.75 g, 1.51 mmol), and caesium carbonate (Cs_2CO_3 , 0.54 g, 1.66 mmol) in dimethyl sulfoxide (DMSO, 4.2 mL) was heated at 130 °C for 9 hours. After completion of the reaction, DMSO was removed by distillation under vacuum. The residue was taken up with dichloromethane. The insoluble salt was removed by filtration through celite. The filtrate was washed with brine. The organic extracts were dried over anhydrous magnesium sulfate and concentrated by rotary evaporation to give crude residue that was further purified by liquid chromatography on silica gel, using hexanes/ethylacetate (10:1) as the eluent to give **5** as yellowish crystals (0.22 g, 21% yield). The product **5** was directly used for preparation of **1-3cbzBIZ**.

^1H NMR (400 MHz, CD_2Cl_2): δ 9.05 (s, 1H), 8.45 (d, J = 8.4 Hz, 1H), 8.18 (d, J = 7.6 Hz, 4H), 7.97-7.94 (m, 3H), 7.63-7.60 (m, 2H), 7.52-7.42 (m, 6H), 7.38-7.36 (m, 4H), 7.32-7.26 (m, 5H), 6.72-6.62 (m, 3H), 6.44 (d, J = 7.6 Hz, 2H); ^{13}C NMR (100 MHz, CD_2Cl_2): δ 142.22, 140.49, 139.32, 139.10, 138.48, 137.68, 130.75, 127.90, 127.72, 127.10, 126.39, 126.34, 126.27, 124.61, 124.33, 123.50, 122.17, 120.64, 120.23, 120.11, 119.84, 119.72, 112.03, 110.04.

9-(1,2-Diphenyl-1*H*-benzo[d]imidazol-7-yl)-9*H*-3,6-di(*N*-carbazolyl)carbazole (1-3cbzBIZ**)**



1-3cbzBIZ

A mixture of **5** (0.28 g, 0.39 mmol), tin(II) chloride (SnCl_2 , 0.37 g, 1.95 mmol), benzaldehyde (0.05 mL) and sodium metabisulfite (0.08 g, 0.46 mmol) in dried dimethylformamide (DMF, 2.2 mL) and ethanol (2.2 mL) was heated at 130 °C for 16 hours. After completion of the reaction, the solvent was removed by distillation under reduced pressure. The residue was taken up with chloroform. The insoluble salt was removed by filtration through celite. The filtrate was washed with brine. The organic extracts were dried over anhydrous magnesium sulfate and concentrated by rotary evaporation to give crude residue that was further purified by liquid chromatography on silica gel, using hexanes/chloroform (1:5) as the eluent to give **1-3cbzBIZ** as colourless crystals (0.29 g, 94% yield)

^1H NMR (400 MHz, CD_2Cl_2): δ 8.22-8.16 (m, 5H), 8.03 (s, 2H), 7.69 (t, J = 7.6 Hz, 1H), 7.60 (d, J = 6.8 Hz, 1H), 7.52-7.33 (m, 13H), 7.32-7.21 (m, 8H), 7.01-6.96 (m, 1H), 6.76-6.70(m, 4H); ^{13}C NMR (100 MHz, CD_2Cl_2): δ 154.35, 146.16, 142.18, 142.05, 135.82, 134.42, 130.24, 130.18, 130.01, 129.95, 128.73, 128.59, 128.11, 127.45, 126.32, 126.15, 125.81, 123.92, 123.73, 123.49, 121.95, 120.83, 120.64, 120.10, 119.57, 111.75, 110.05. HRMS (MALDI-TOF) m/z calcd for $\text{C}_{55}\text{H}_{35}\text{N}_5$ 765.2892, obsd. 765.2916. Anal. Calcd for $\text{C}_{55}\text{H}_{35}\text{N}_5$: C, 86.25; H, 4.61; N, 9.14; Found: C, 86.03; H, 4.46; N, 9.14.

Fig. S1. ^1H NMR spectrum of **5**

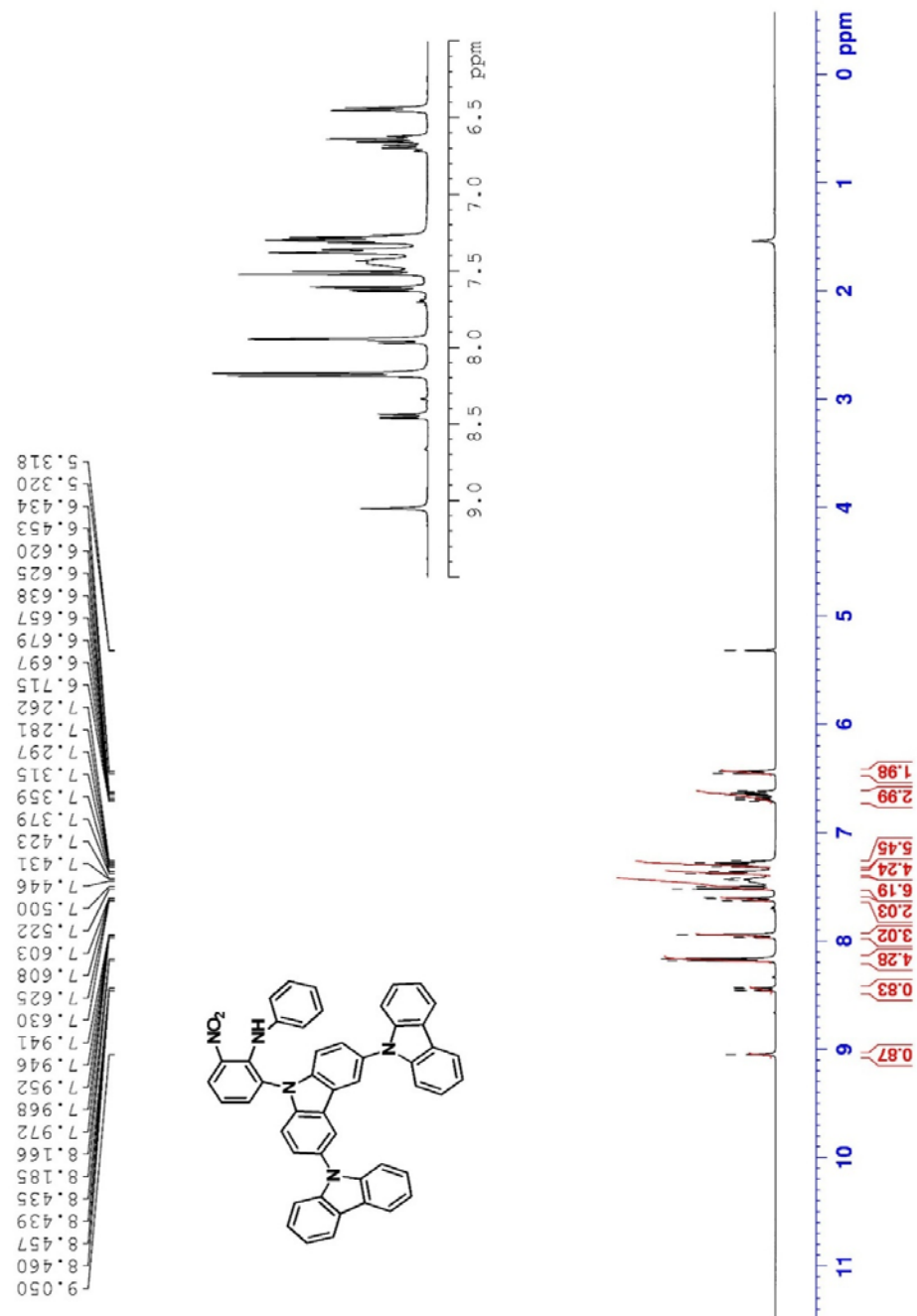


Fig. S2. ^{13}C NMR spectrum of **5**

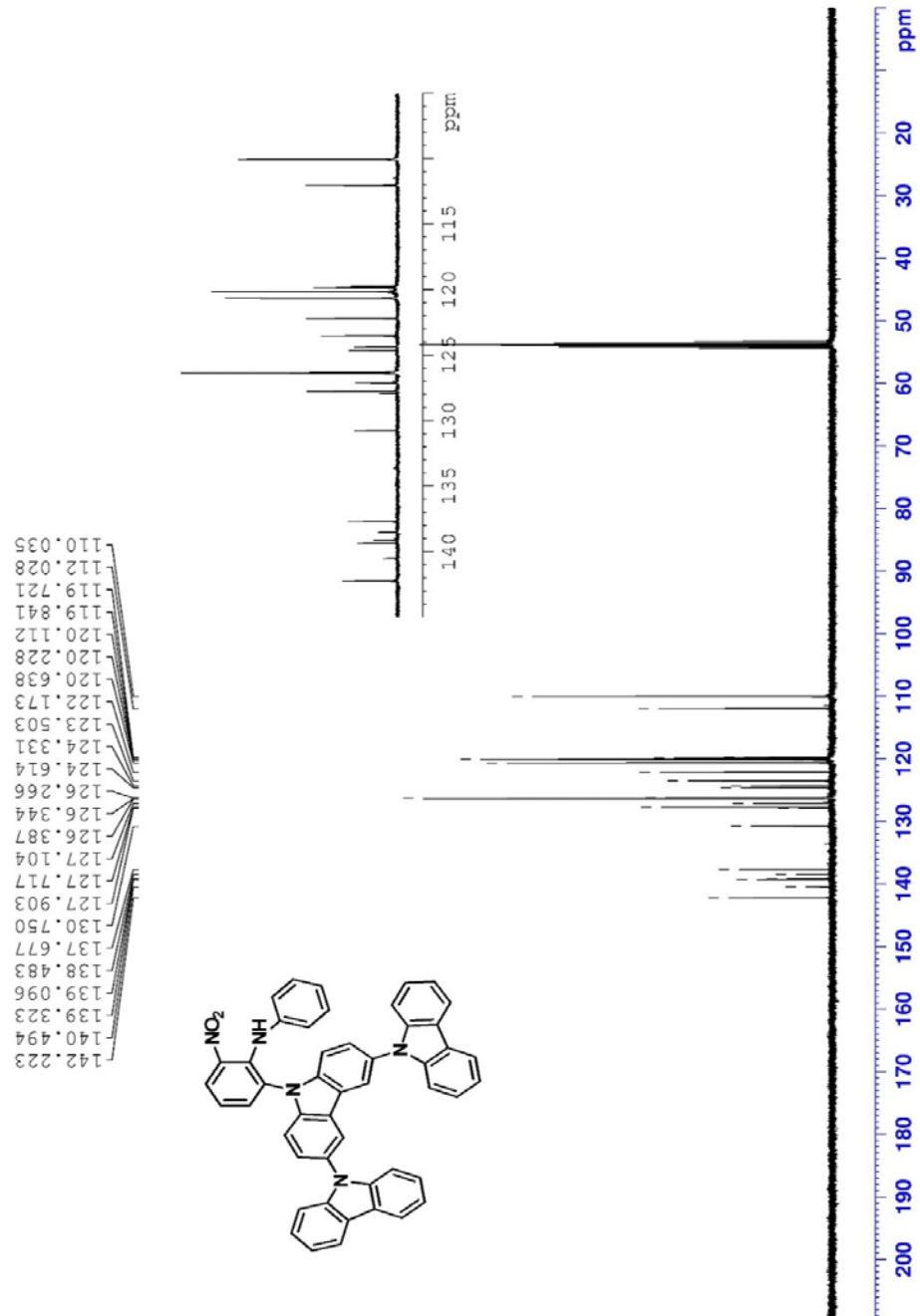


Fig. S3. ^1H NMR spectrum of **4-3cbzBIZ**

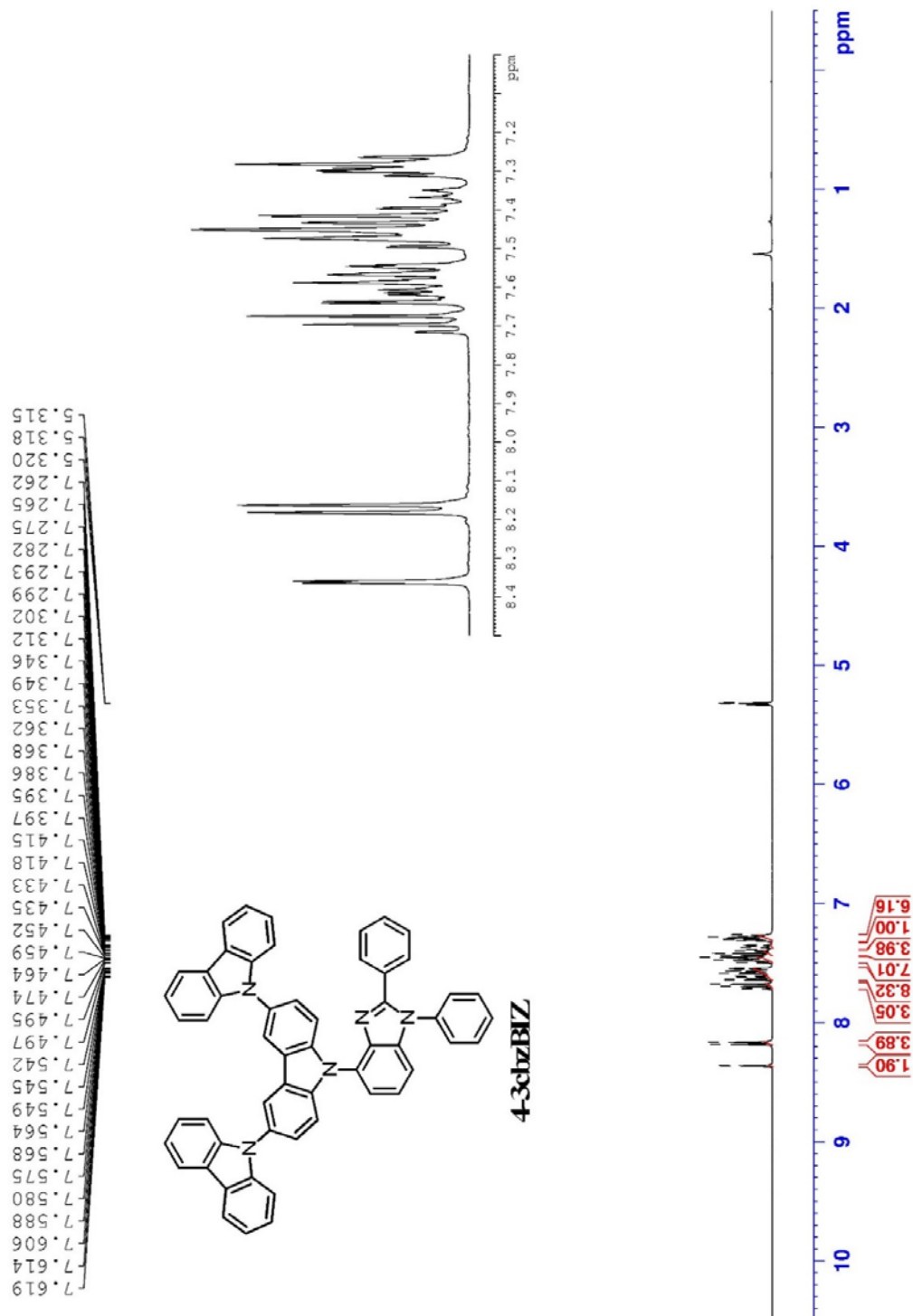


Fig. S4. ^{13}C NMR spectrum of **4-3cbzBIZ**

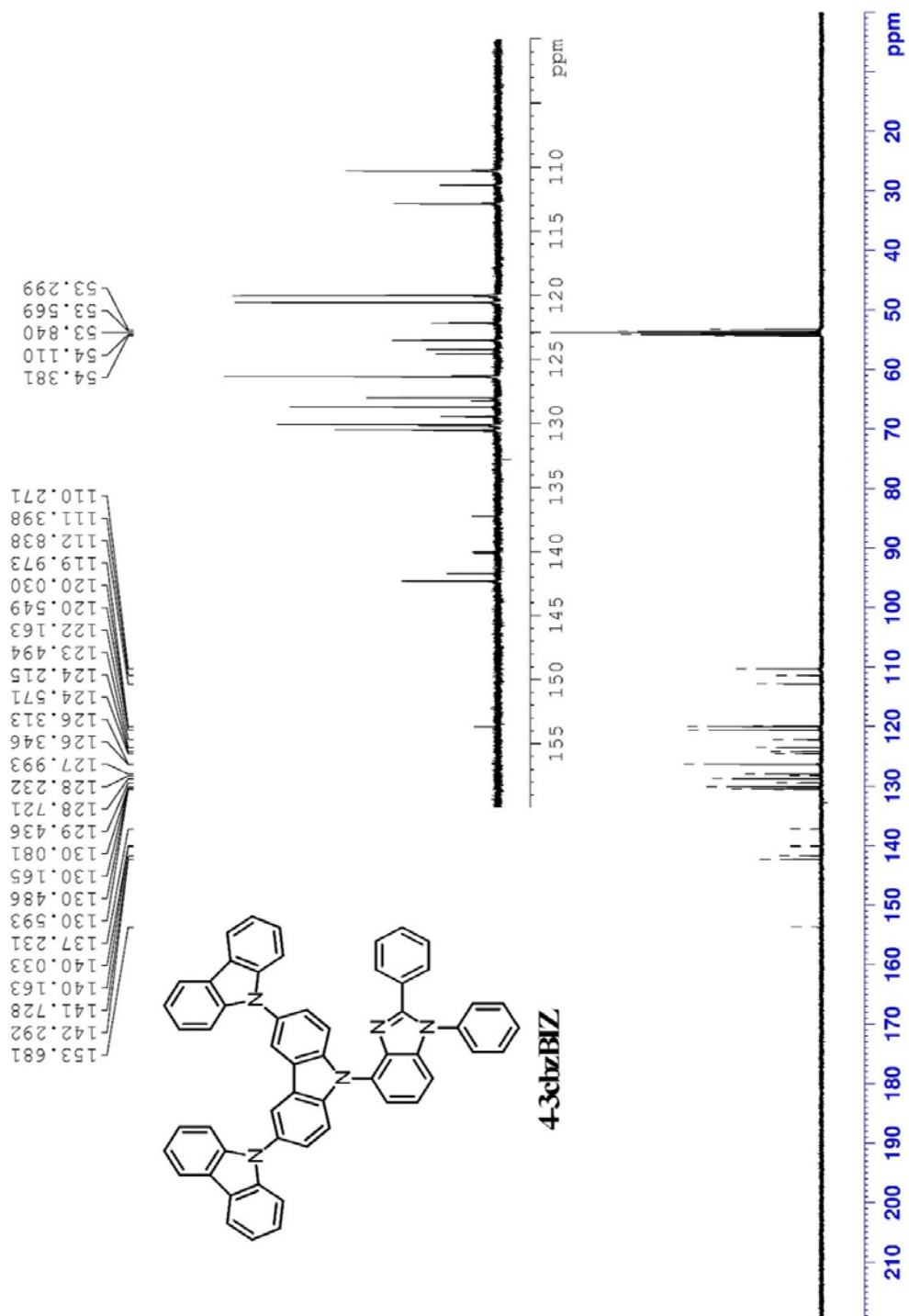


Fig. S5. ^1H NMR spectrum of **3-3cbzBIZ**

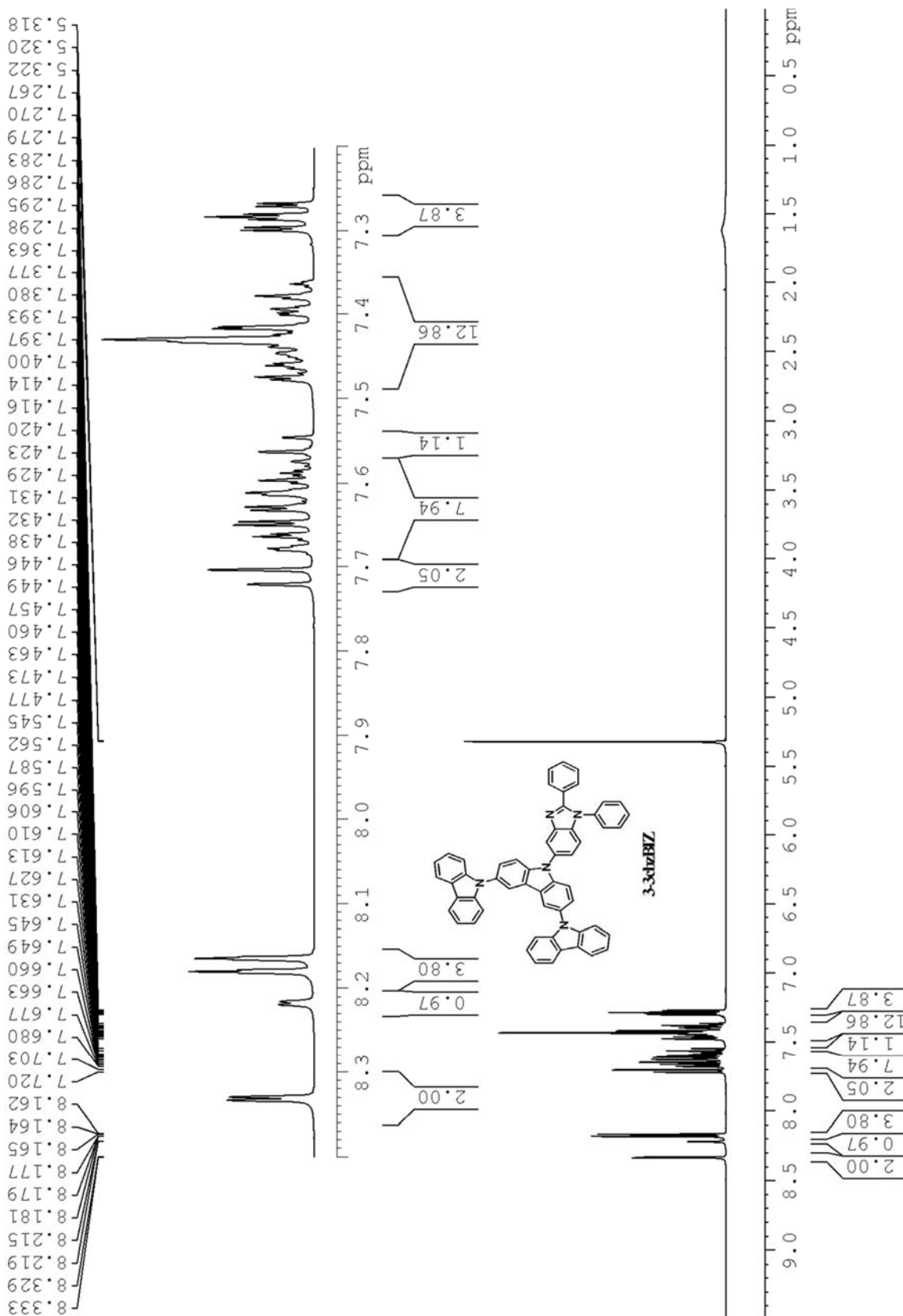


Fig. S6. ^{13}C NMR spectrum of **3-3cbzBIZ**

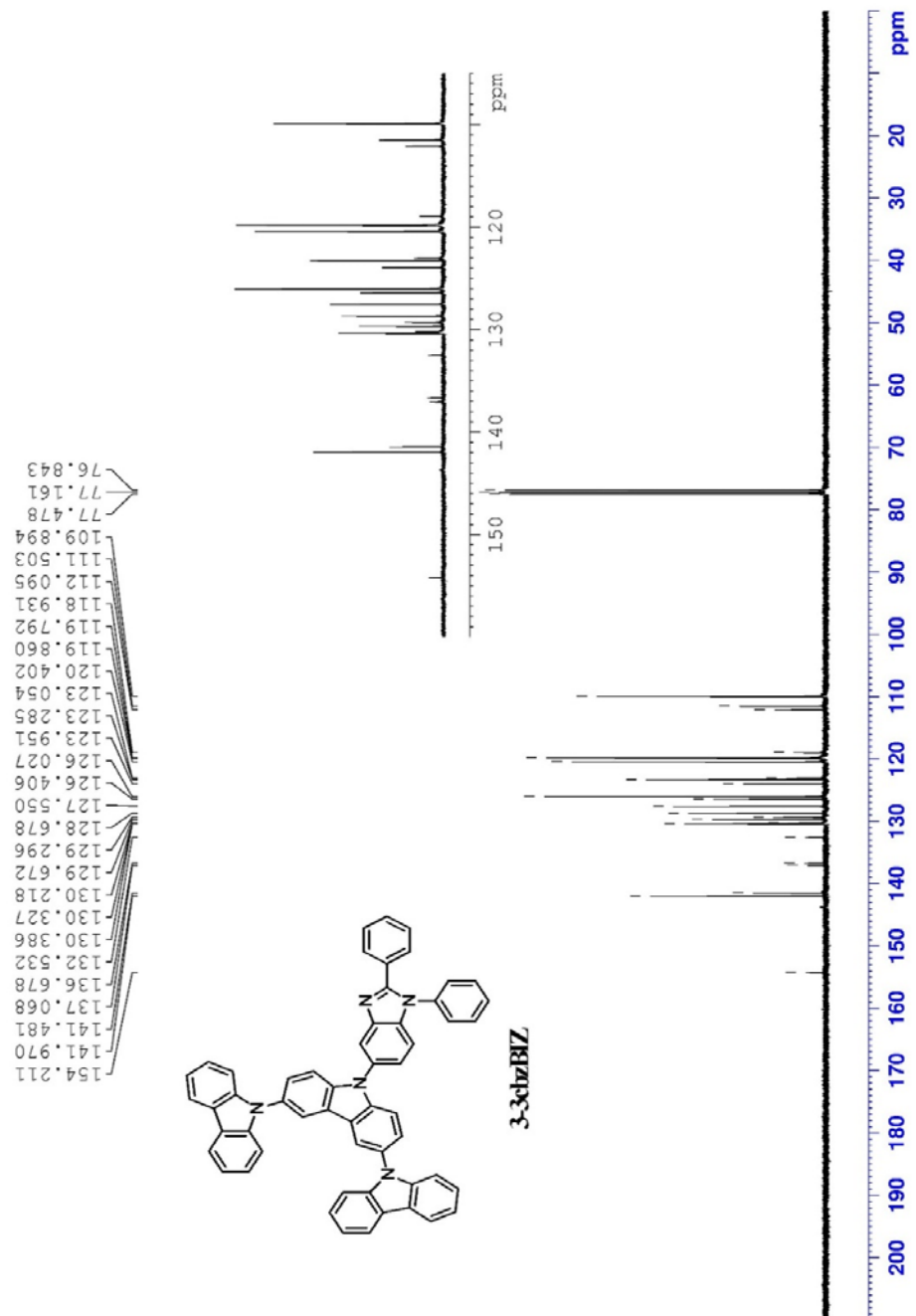


Fig. S7. ^1H NMR spectrum of **2-3cbzBIZ**

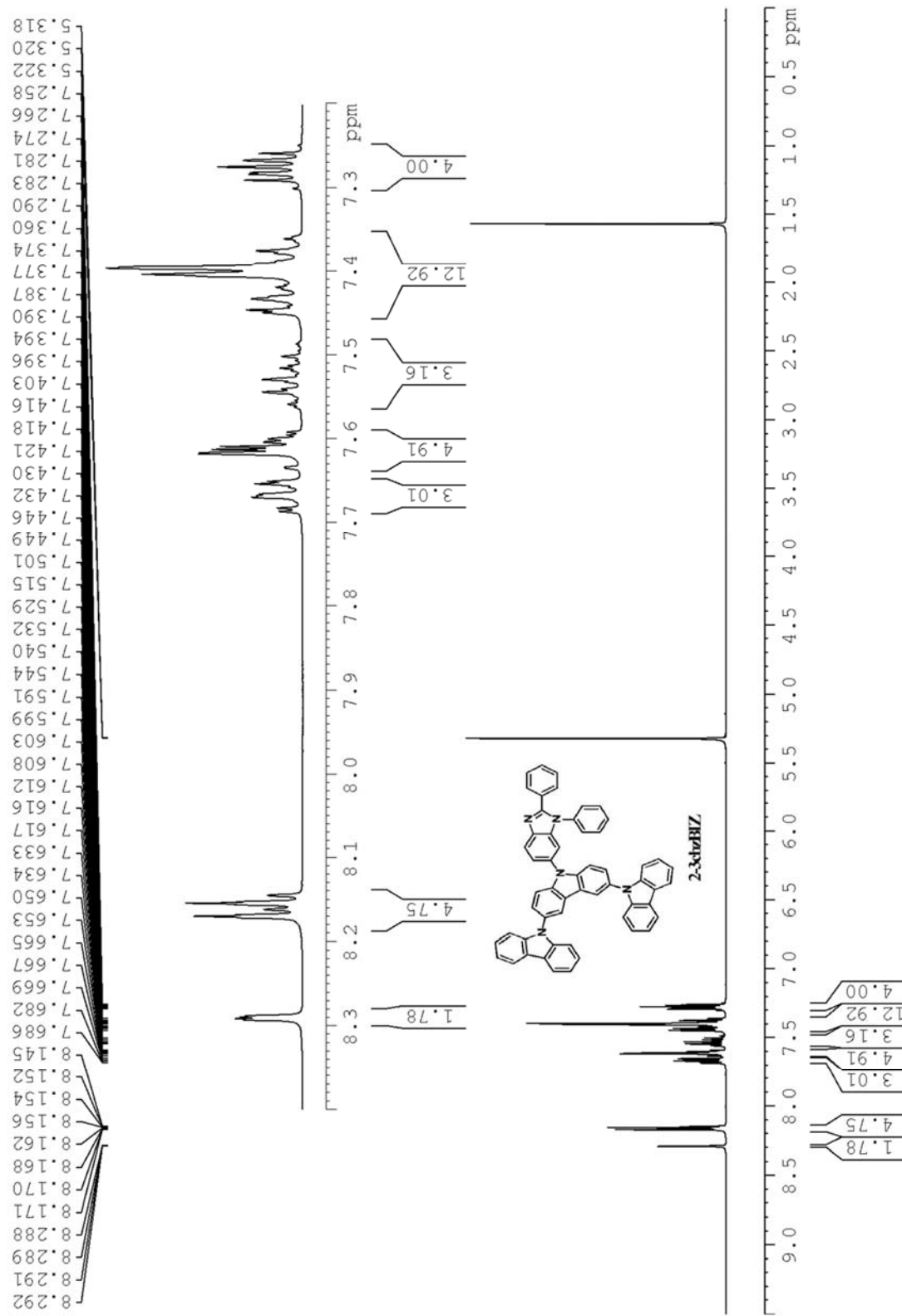


Fig. S8. ^{13}C NMR spectrum of 2-3cbzBIZ

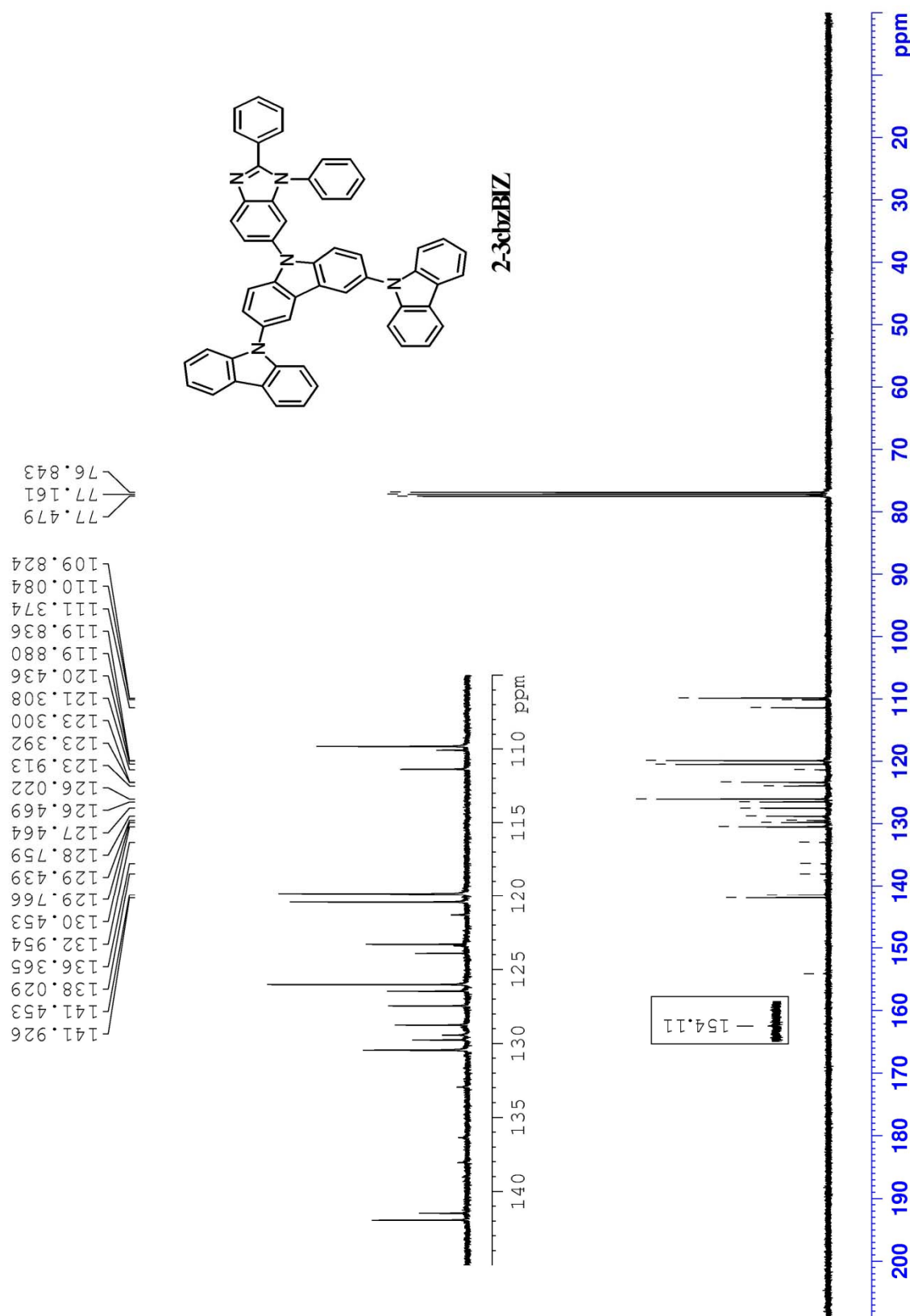


Fig. S9. ^1H NMR spectrum of **1-3cbzBIZ**

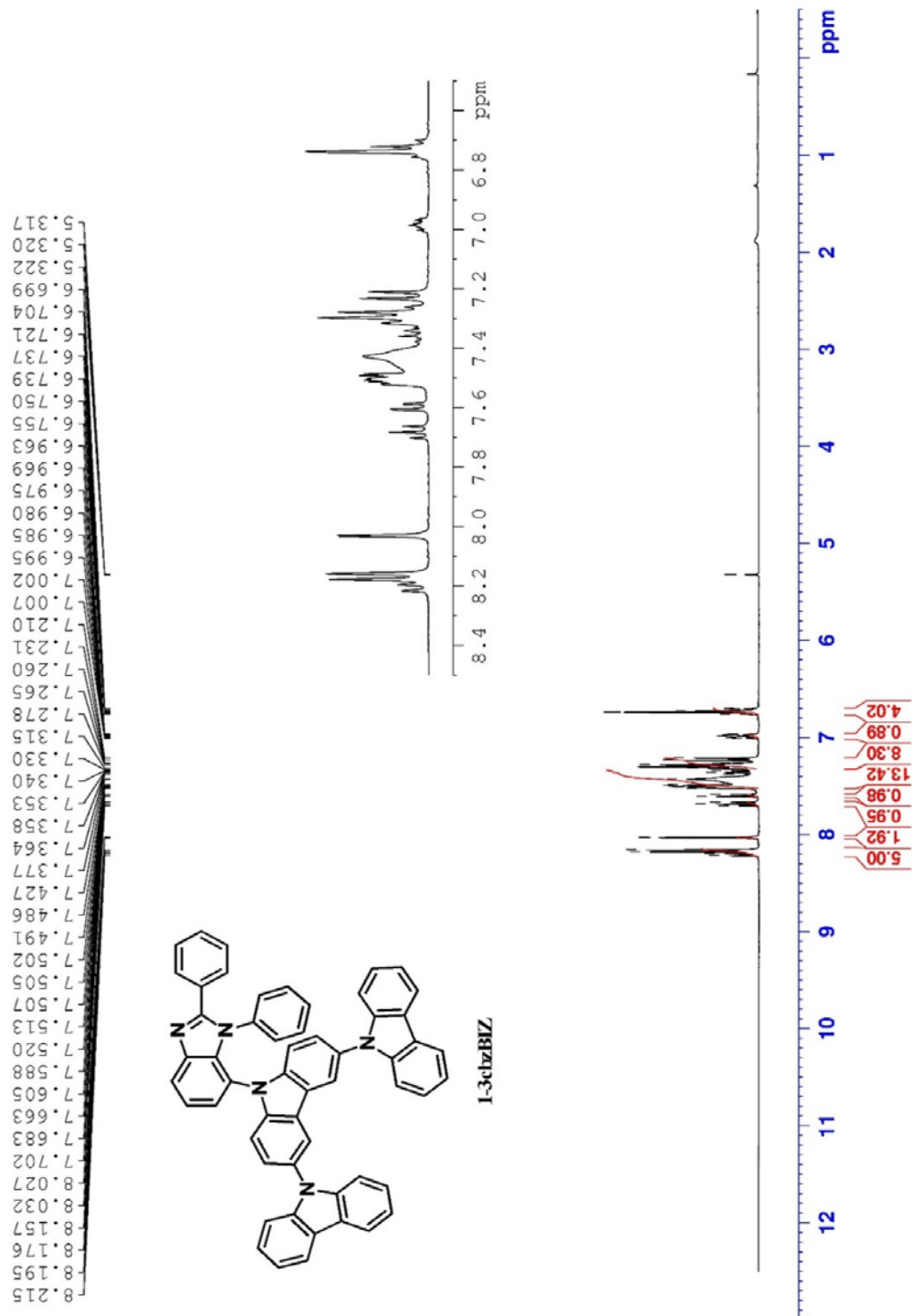


Fig. S10. ^{13}C NMR spectrum of **1-3cbzBIZ**

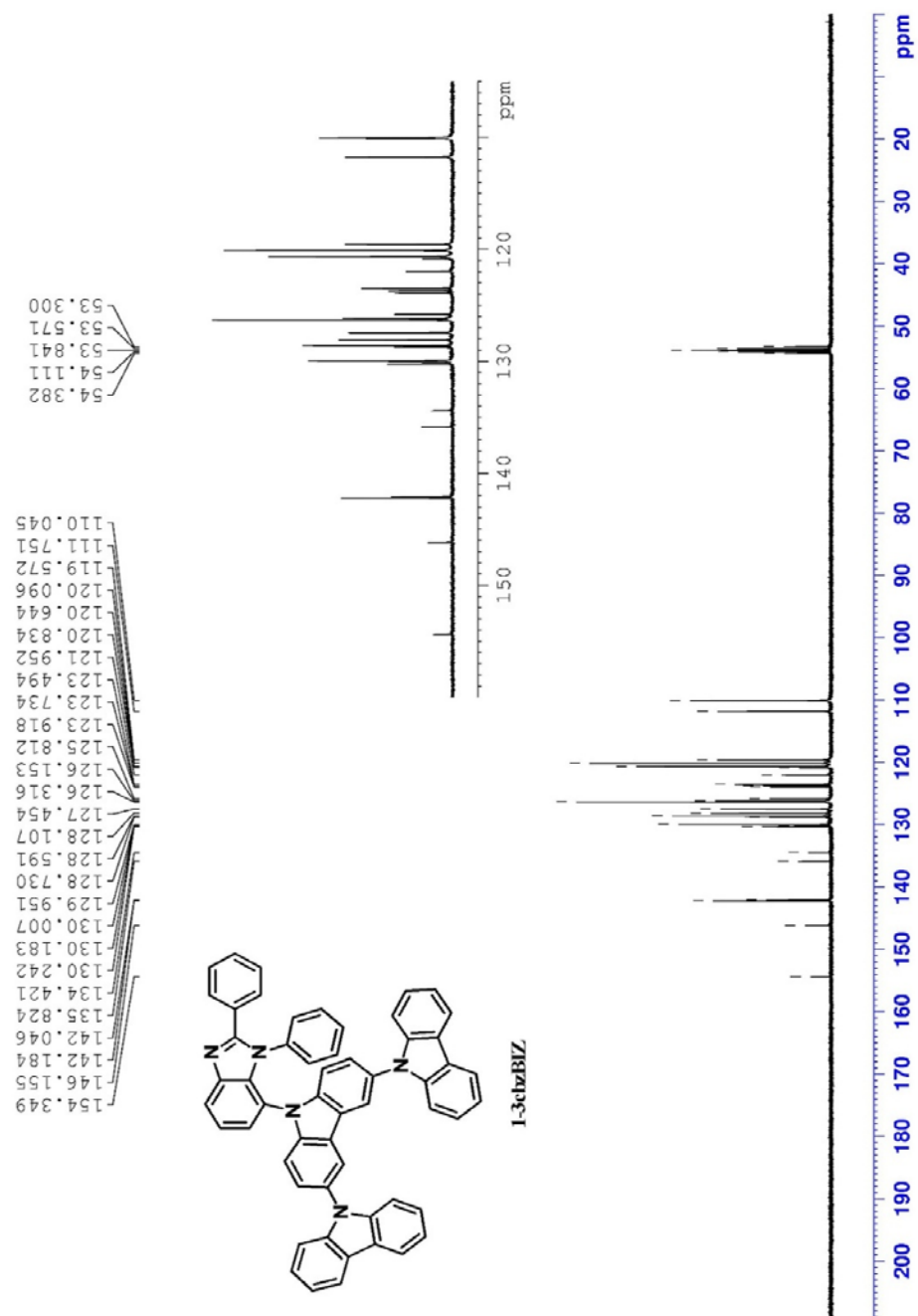


Fig. S11. ORTEP of 1-3cbzBIZ

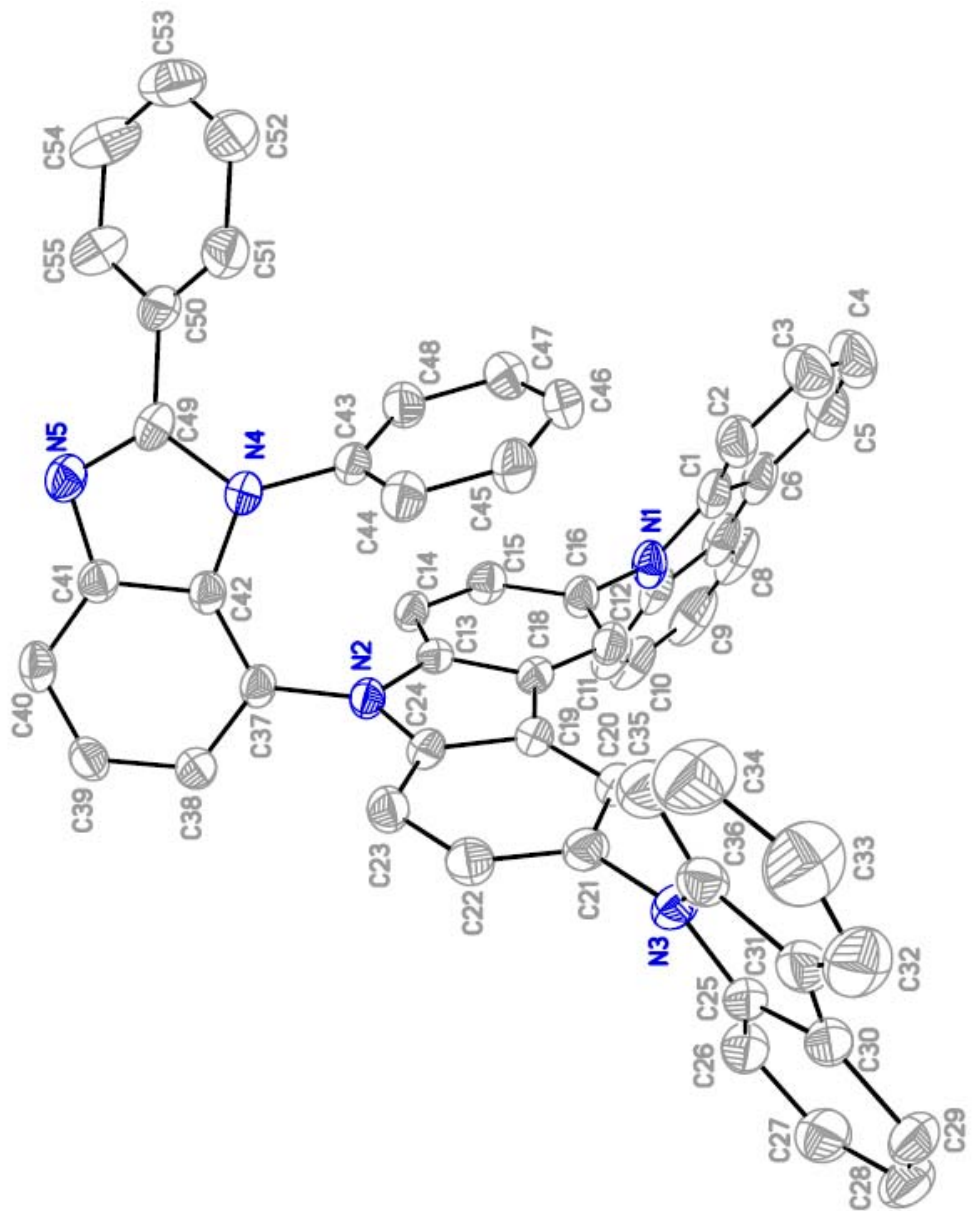


Table S1. Crystal data and experimental details for **1-3cbzBIZ** (ic19209).

Crystal data		
Empirical formula	C57 H35 N5 O	
Formula weight	805.90	
Crystal system	Triclinic	
Space group	P-1	
Unit cell dimensions	a = 9.5409(6) Å b = 12.4732(7) Å c = 19.1087(7) Å	$\alpha = 106.064(4)^\circ$. $\beta = 91.848(4)^\circ$. $\gamma = 104.015(5)^\circ$.
Volume	2108.15(19) Å ³	
Z	2	
F(000)	840	
Density (calculated)	1.270 Mg/m ³	
Wavelength	0.71073 Å	
Cell parameters reflections used	4336	
Theta range for Cell parameters	3.3450 to 28.2410°.	
Absorption coefficient	0.077 mm ⁻¹	
Temperature	150(2) K	
Crystal size	0.25 x 0.20 x 0.15 mm ³	
Data collection		
Diffractometer	Xcalibur, Atlas, Gemini	
Absorption correction	Semi-empirical from equivalents	
Max. and min. transmission	1.00000 and 0.98521	
No. of measured reflections	13093	
No. of independent reflections	7393 [R(int) = 0.0396]	
No. of observed [I>2_igma(I)]	4926	
Completeness to theta = 25.00°	99.5 %	
Theta range for data collection	3.10 to 25.00°.	
Refinement		
Final R indices [I>2sigma(I)]	R1 = 0.0526, wR2 = 0.1101	
R indices (all data)	R1 = 0.0904, wR2 = 0.1346	
Goodness-of-fit on F ²	1.020	
No. of reflections	7393	
No. of parameters	583	
No. of restraints	0	
Largest diff. peak and hole	0.393 and -0.272 e.Å ⁻³	

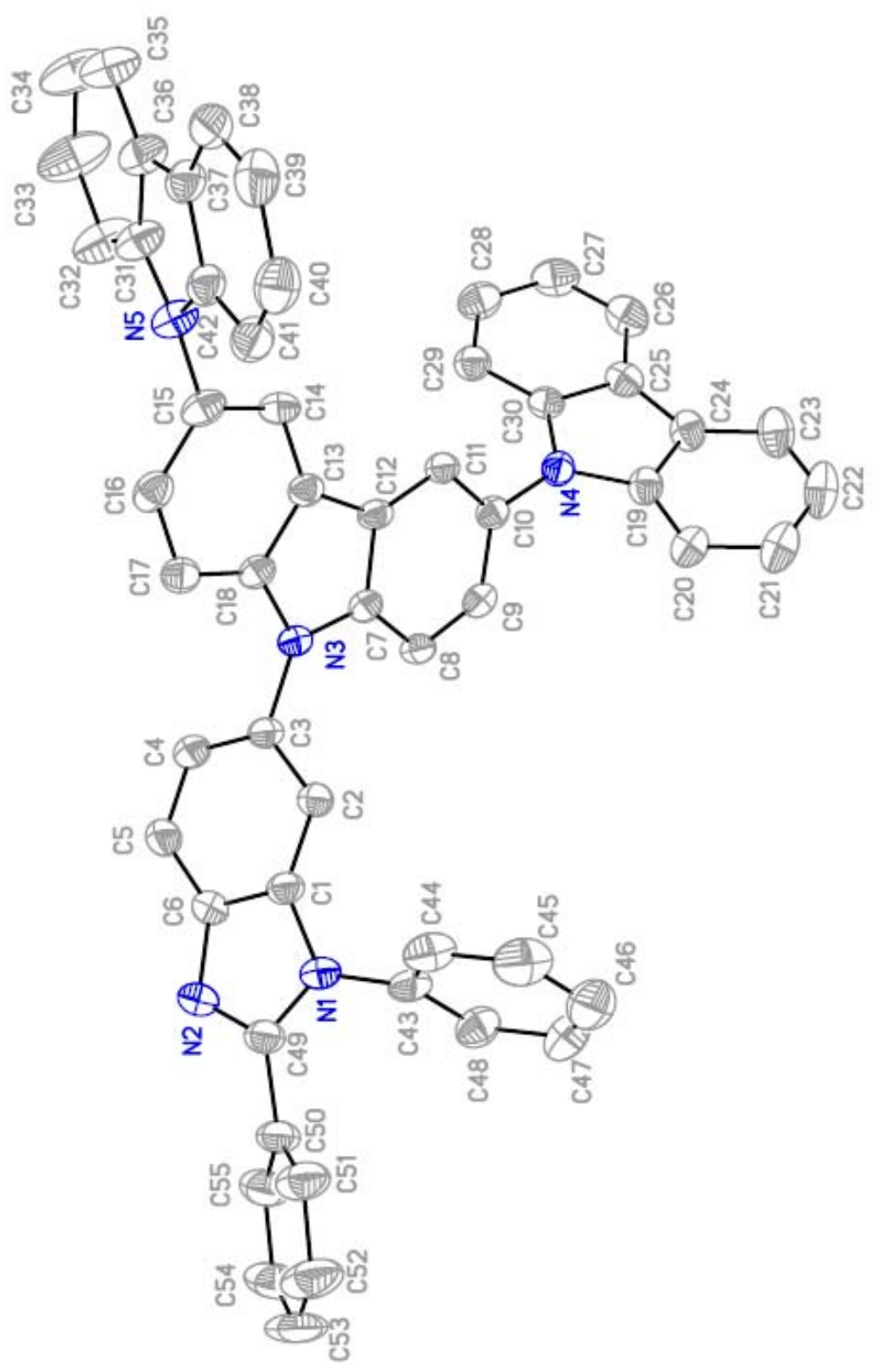


Fig. S12. ORTEP of **2-3cbzBIZ**

Table S2. Crystal data and structure refinement for ic18894.

Identification code	ic18894		
Empirical formula	C56 H37 Cl2 N5		
Formula weight	850.81		
Temperature	150(2) K		
Wavelength	1.54178 Å		
Crystal system	Monoclinic		
Space group	P 1 21/c 1		
Unit cell dimensions	$a = 16.6376(6)$ Å	$\alpha = 90^\circ$.	
	$b = 19.3882(7)$ Å	$\beta = 102.484(4)^\circ$.	
	$c = 13.5075(5)$ Å	$\gamma = 90^\circ$.	
Volume	4254.1(3) Å ³		
Z	4		
Density (calculated)	1.328 Mg/m ³		
Absorption coefficient	1.730 mm ⁻¹		
F(000)	1768		
Crystal size	0.20 x 0.15 x 0.10 mm ³		
Theta range for data collection	3.55 to 68.00°.		
Index ranges	-18<=h<=20, -23<=k<=14, -16<=l<=16		
Reflections collected	19842		
Independent reflections	7748 [R(int) = 0.0371]		
Completeness to theta = 68.00°	99.9 %		
Absorption correction	Semi-empirical from equivalents		
Max. and min. transmission	1.00000 and 0.88409		
Refinement method	Full-matrix least-squares on F ²		
Data / restraints / parameters	7748 / 0 / 568		
Goodness-of-fit on F ²	1.032		
Final R indices [I>2sigma(I)]	R1 = 0.0514, wR2 = 0.1349		
R indices (all data)	R1 = 0.0709, wR2 = 0.1506		
Largest diff. peak and hole	0.527 and -0.568 e.Å ⁻³		

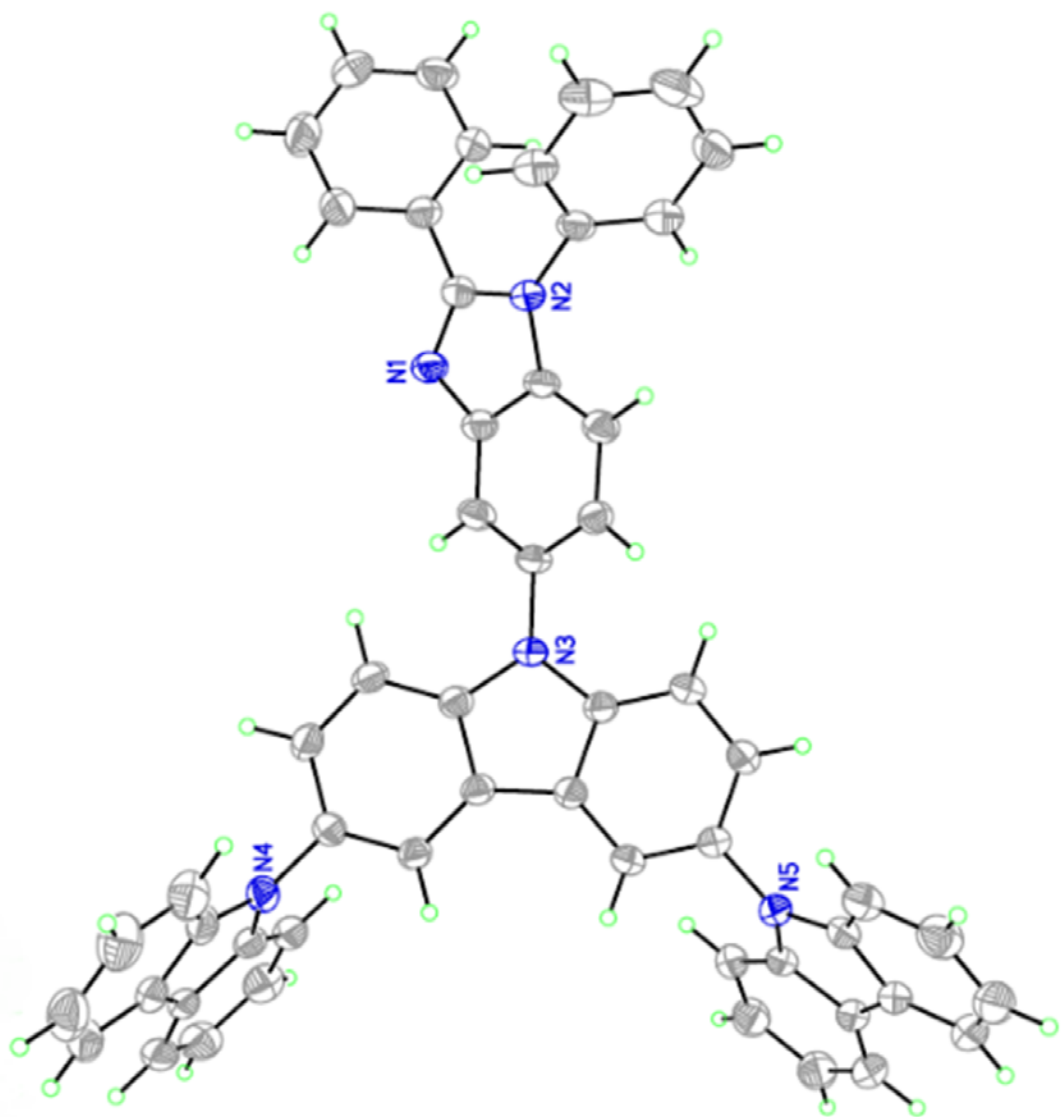


Fig. S13 ORTEP of **3-3cbzBIZ**

Table S3. Crystal data and structure refinement for ic18971.

Identification code	ic18971		
Empirical formula	C58 H41 N5 O		
Formula weight	823.96		
Temperature	200(2) K		
Wavelength	0.71073 Å		
Crystal system	Triclinic		
Space group	P -1		
Unit cell dimensions	$a = 12.9028(5)$ Å	$\alpha = 63.011(5)$ °.	
	$b = 13.7936(6)$ Å	$\beta = 73.842(4)$ °.	
	$c = 14.0702(8)$ Å	$\gamma = 86.730(3)$ °.	
Volume	2136.27(17) Å ³		
Z	2		
Density (calculated)	1.281 Mg/m ³		
Absorption coefficient	0.077 mm ⁻¹		
F(000)	864		
Crystal size	0.350 x 0.150 x 0.080 mm ³		
Theta range for data collection	2.96 to 27.50°.		
Index ranges	-16≤h≤16, -13≤k≤17, -18≤l≤17		
Reflections collected	15875		
Independent reflections	9339 [R(int) = 0.0297]		
Completeness to theta = 27.50°	95.3 %		
Absorption correction	Semi-empirical from equivalents		
Max. and min. transmission	1.00000 and 0.98201		
Refinement method	Full-matrix least-squares on F ²		
Data / restraints / parameters	9339 / 0 / 577		
Goodness-of-fit on F ²	1.016		
Final R indices [I>2sigma(I)]	R1 = 0.0552, wR2 = 0.1184		
R indices (all data)	R1 = 0.0915, wR2 = 0.1410		
Largest diff. peak and hole	0.557 and -0.284 e.Å ⁻³		

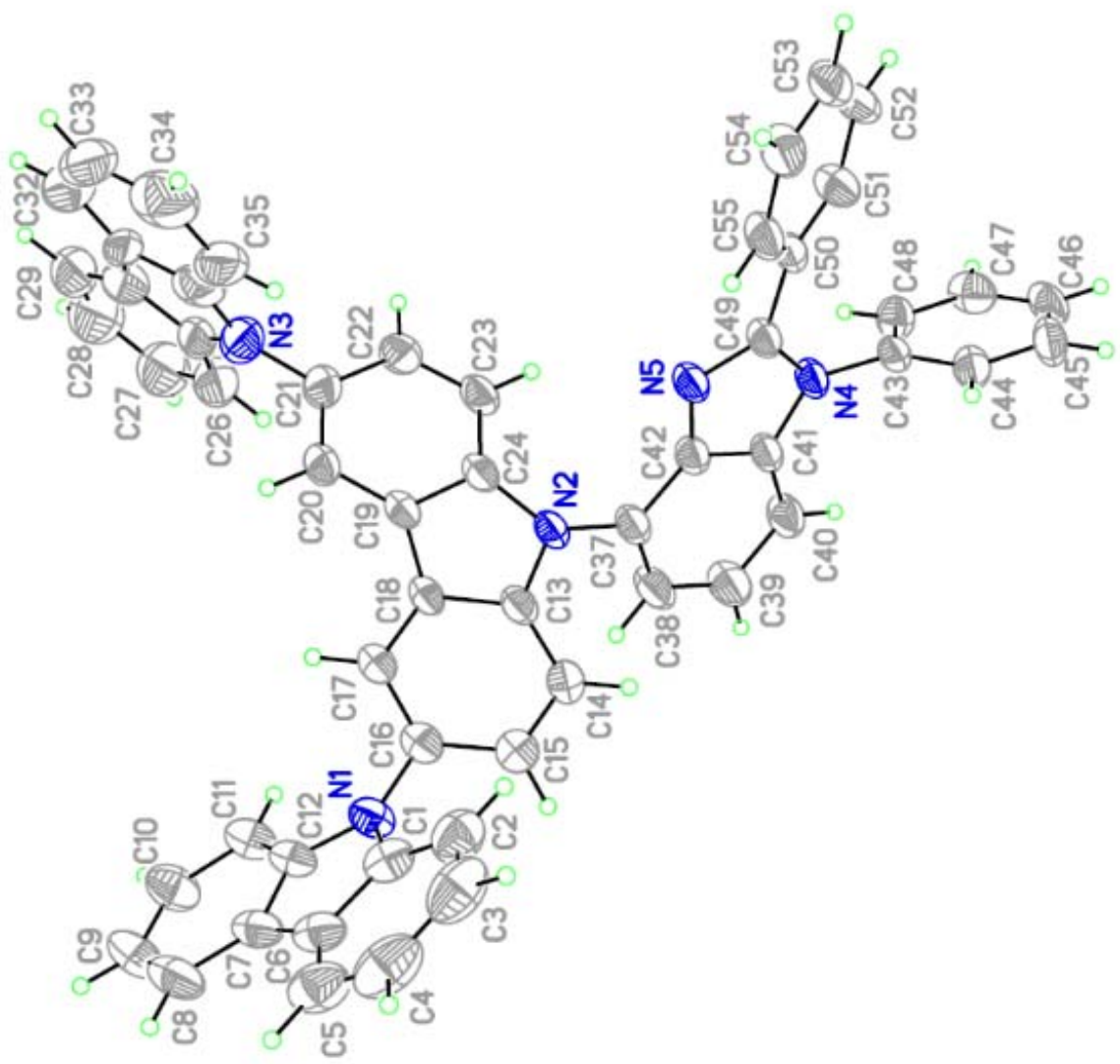


Fig. S14. ORTEP of 4-3cbzBIZ

Table S4. Crystal data and structure refinement for ic18783.

Identification code	ic18783	
Empirical formula	C55.50 H36 Cl N5	
Formula weight	808.34	
Temperature	200(2) K	
Wavelength	0.71073 Å	
Crystal system	Monoclinic	
Space group	P2(1)/n	
Unit cell dimensions	$a = 13.0717(3)$ Å	$\alpha = 90^\circ$.
	$b = 13.8814(3)$ Å	$\beta = 90.645(2)^\circ$.
	$c = 23.1396(5)$ Å	$\gamma = 90^\circ$.
Volume	4198.50(16) Å ³	
Z	4	
Density (calculated)	1.279 Mg/m ³	
Absorption coefficient	0.137 mm ⁻¹	
F(000)	1684	
Crystal size	0.25 x 0.20 x 0.15 mm ³	
Theta range for data collection	2.78 to 27.50°.	
Index ranges	-16<=h<=16, -18<=k<=18, -28<=l<=26	
Reflections collected	28993	
Independent reflections	9330 [R(int) = 0.0401]	
Completeness to theta = 27.50°	96.9 %	
Absorption correction	Semi-empirical from equivalents	
Max. and min. transmission	1.00000 and 0.98811	
Refinement method	Full-matrix least-squares on F ²	
Data / restraints / parameters	9330 / 0 / 568	
Goodness-of-fit on F ²	1.009	
Final R indices [I>2sigma(I)]	R1 = 0.0635, wR2 = 0.1593	
R indices (all data)	R1 = 0.1081, wR2 = 0.1926	
Largest diff. peak and hole	0.568 and -0.329 e.Å ⁻³	

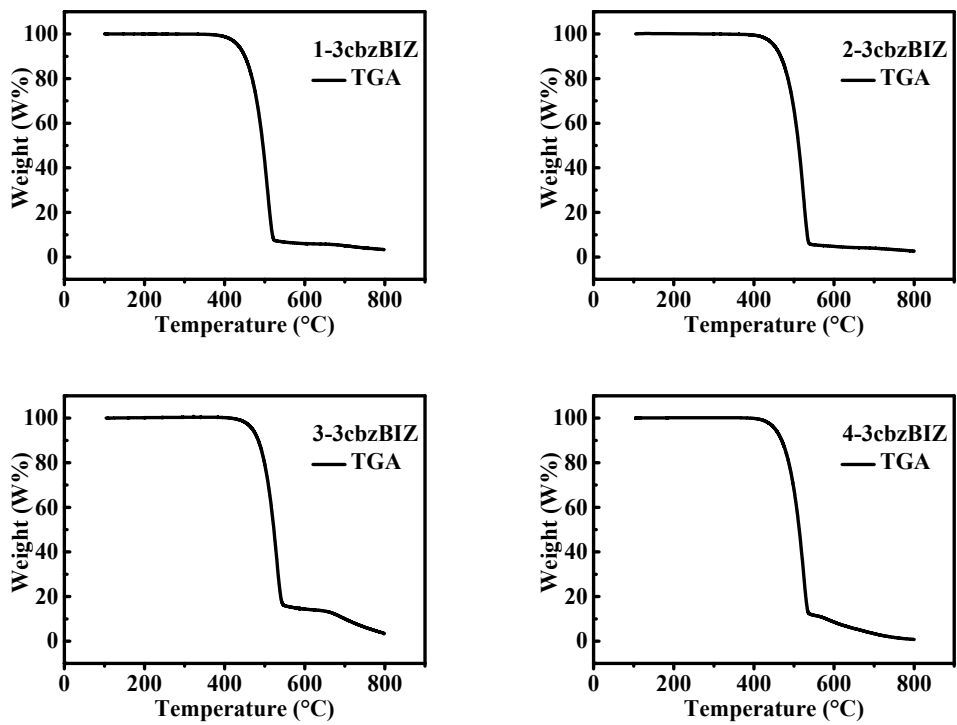


Fig. S15. Thermogravimetric analysis of **3cbzBIZ's**

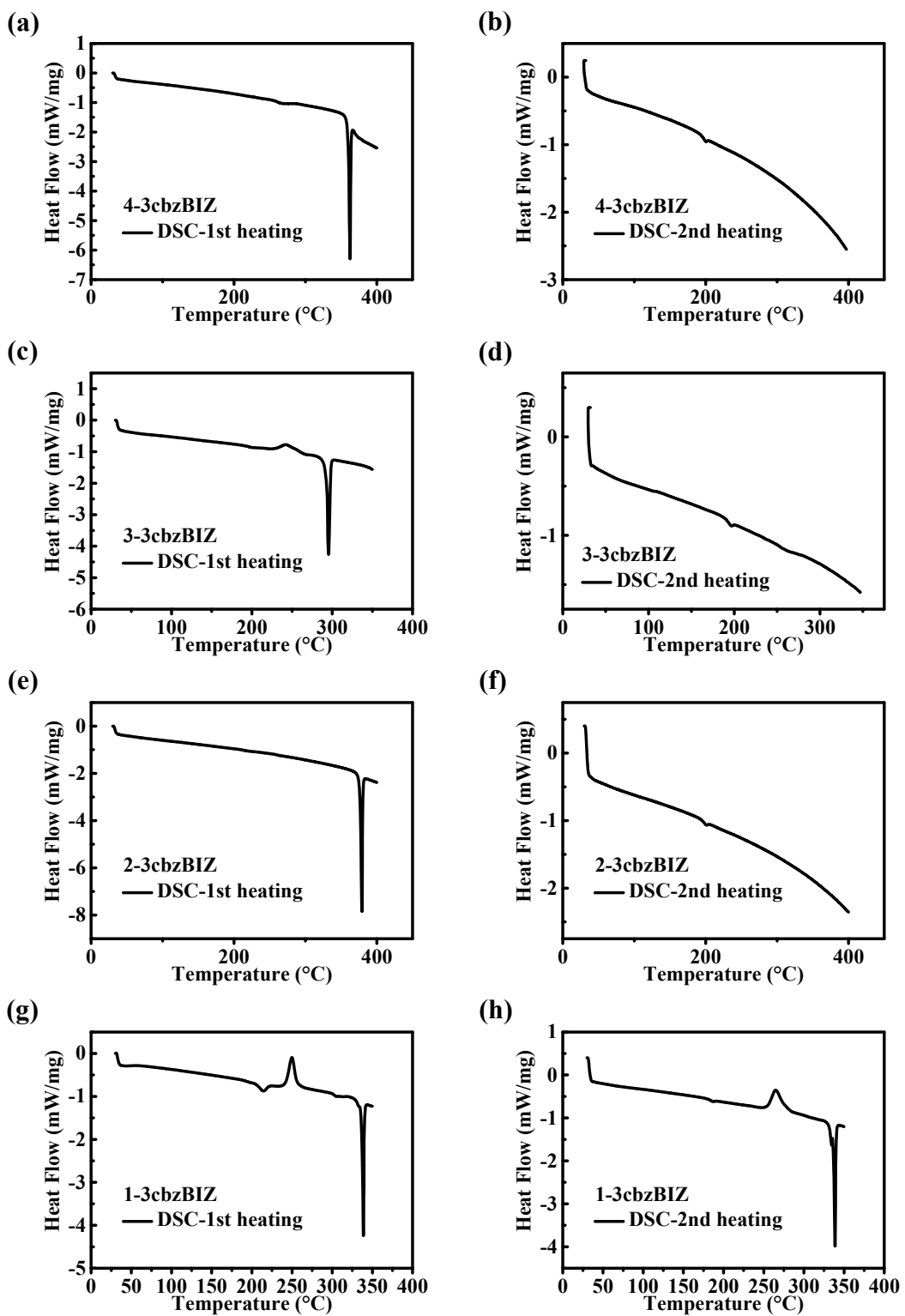


Fig. S16. Differential scanning calorimetric analysis of 3cbzBIZ's

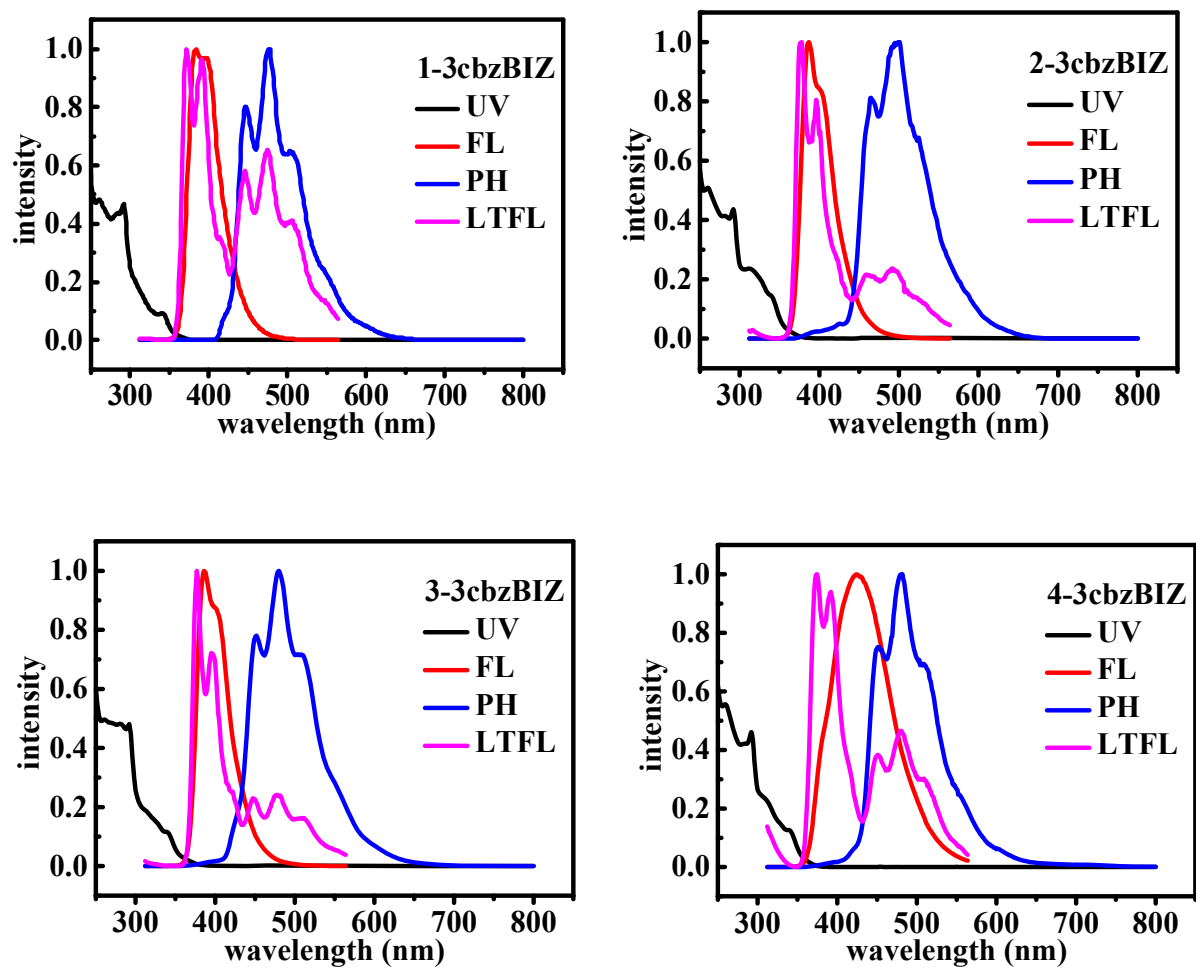


Fig. S17. Spectrometric analysis of **3cbzBIZ**'s, including UV-Vis, room temperature steady state fluorescence, and low temperature fluorescence and phosphorescence spectral data at 77K

The initial structures for the **3cbzBIZ**'s were first setup based on their crystal structures. These structures have undergone geometry optimizations through density functional theory (DFT) calculations (DA) at the S₀ state. In these DFT-based optimizations, the BLYP-D3/6-311+G(d)³⁻⁶ hybrid functional was used.

Table S5. The theoretical HOMO and LUMO information of **3cbzBIZ**'s in THF was predicted by the Ab initio calculation method at BLYP-D3/6-311+G(d) level.

	1-3cbzBIZ		2-3cbzBIZ		3-3cbzBIZ		4-3cbzBIZ	
	Calcd (ev)	Exptl ^a (ev)	Calcd (ev)	Exptl (ev)	Calcd (ev)	Exptl (ev)	Calcd (ev)	Exptl (ev)
LUMO	-1.70	-2.41	-1.80	-2.42	-1.80	-2.43	-1.85	-2.41
HOMO	-5.54	-5.78	-5.44	-5.82	-5.38	-5.81	-5.34	-5.78
Optical gap	3.84	3.37	3.64	3.40	3.58	3.38	3.49	3.37

a. In THF

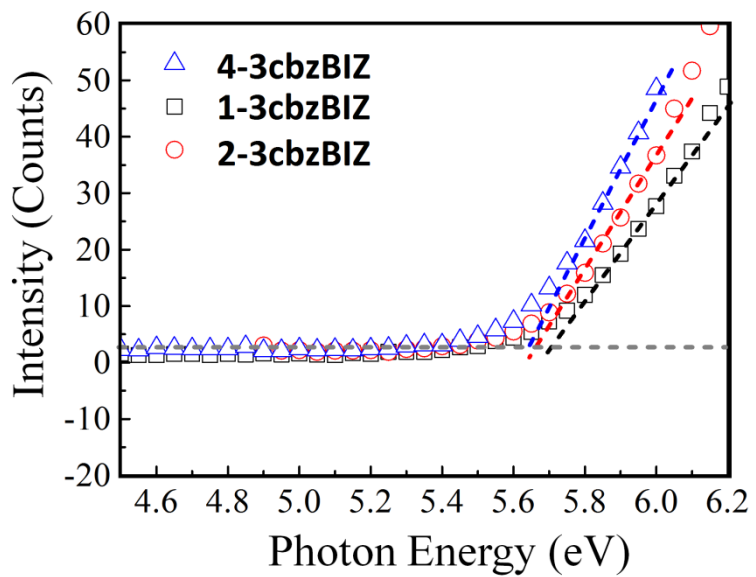


Fig. S18 Photoelectron spectra of **1**-, **2**-, and **4-3cbzBIZ** from AC2 measurements.

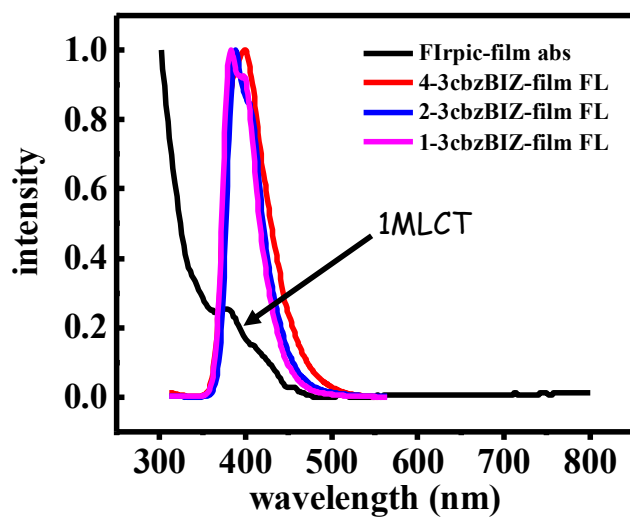


Fig. S19 Photoluminescence spectra of **1**-, **2**-, and **4-3cbzBIZ** and the absorption spectrum of **FIrpic**.

Table S6 Device structure of device B-1 to B-5.

Device	HTL	EBL	EML	ETL	EIL	Cathode
	TAPC	mCP	1-3cbzBIZ : FIrpic	DPPS	LiF	Al
B-1				12%		
B-2		50	10	30	15%	55
B-3					18%	1.5
B-4						50
B-5				30	15%	60

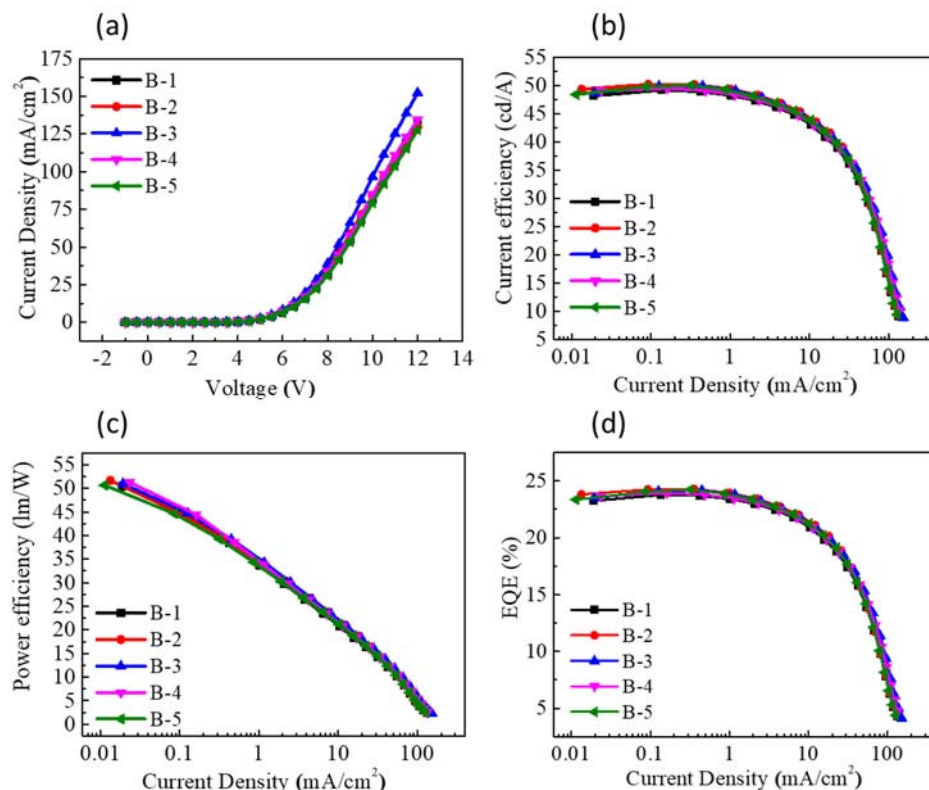


Fig. S20 Device performance of (a) J-V; (b)CE-J; (c)PE-J; (d) EQE-J for device B-1 to B-5 using 1-3cbzBIZ as host.

Table S7 Device performance for device B-1 to B-5.

Device	Driving voltage*	Max. luminance (cd/m ²)	Max. current efficiency (cd/A)	Max. power efficiency (lm/W)	Max. EQE (%)
B-1	7.29	17050	49.17	50.44	23.77
B-2	7.11	17670	50.15	51.66	24.28
B-3	7.00	19550	49.84	50.98	24.18
B-4	7.11	18700	49.50	51.29	23.92
B-5	7.30	17030	49.74	50.66	24.04

Table S8 Device structure of devices C-1 to C-5.

Device	HTL	EBL	EML	ETL	EIL	Cathode
	TAPC	mCP	2-3cbzBIZ : Flrpic	DPPS	LiF	Al
C-1				9%		
C-2	50	10	30	12%	50	
C-3				15%		1.5
C-4			30	12%		45
C-5						55

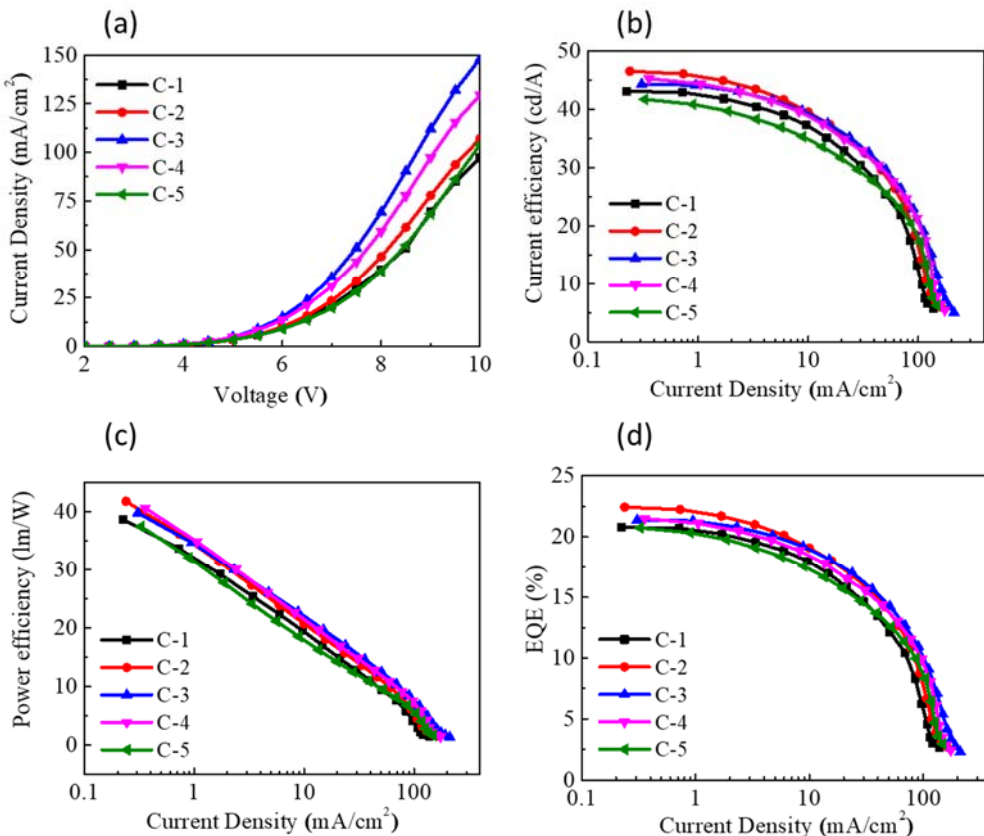


Fig. S21 Device performance of (a) J-V; (b)CE-J; (c)PE-J; (d) EQE-J for devices C-1 to C-5 using 2-3cbzBIZ as host.

Table S9 Device performance for devices C-1 to C-5.

Device	Driving voltage*	Max. luminance (cd/m ²)	Max. current efficiency (cd/A)	Max. power efficiency (lm/W)	Max. EQE (%)
C-1	6.90	15230	43.05	38.64	20.78
C-2	6.75	17730	46.49	41.73	22.42
C-3	6.27	21390	44.26	39.73	21.35
C-4	6.42	17340	45.21	40.58	21.46
C-5	7.01	15810	41.68	37.42	20.73

Table S10 Device structure of devices D-1 to D-7.

Device	HTL	EBL	EML		ETL	EIL	Cathode
	TAPC	mCP	4-3cbzBIZ : FIrpic		DPPS	LiF	Al
D-1				9%			
D-2			30		12%	55	
D-3					15%		
D-4	50	10	30		50	1.5	120
D-5					60		
D-6			40	12%			
D-7			50		55		

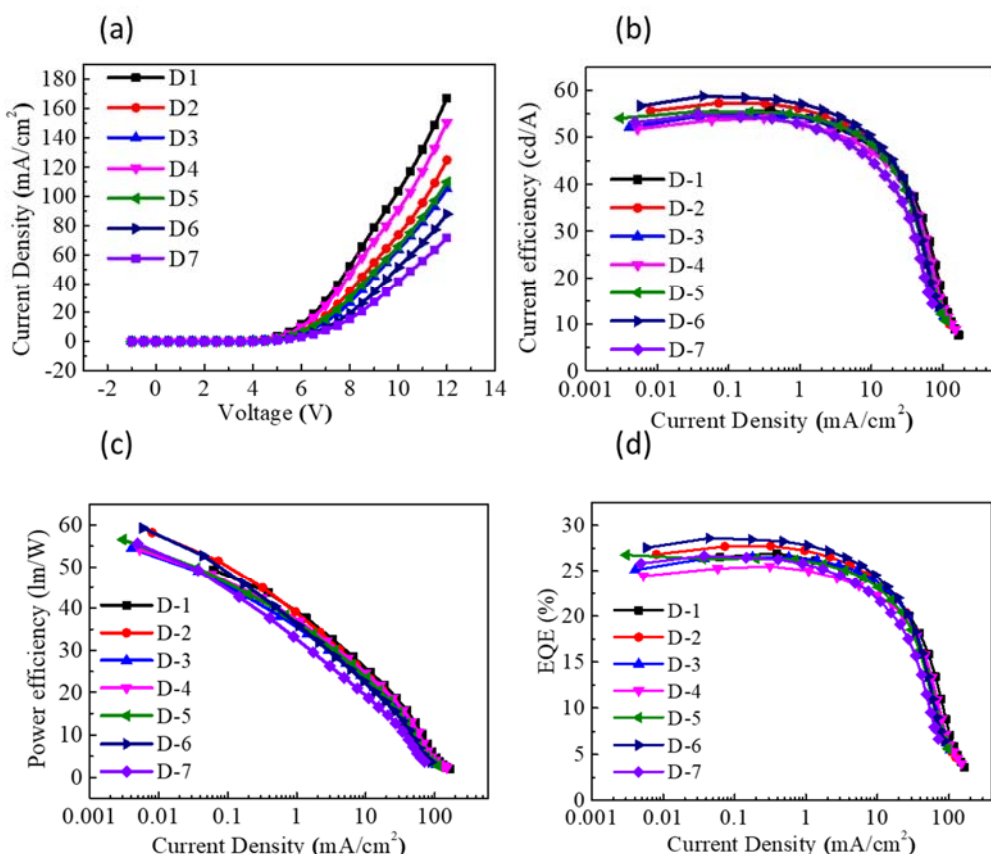


Fig. S22 Device performance of (a) J-V; (b)CE-J; (c)PE-J; (d) EQE-J for device C-1 to C-5 using 4-3cbzBIZ as host.

Table S11 Device performance for devices D-1 to D-7.

Device	Driving voltage*	Max. luminance	Max. current efficiency	Max. power efficiency	Max. EQE
	(V)	(cd/m²)	(cd/A)	(lm/W)	(%)
D-1	6.56	18200	55.71	49.28	26.93
D-2	7.14	15200	57.26	58.15	27.73
D-3	7.56	15170	54.59	54.44	26.51
D-4	6.70	16500	54.03	54.14	25.50
D-5	7.32	13990	55.41	56.55	26.34
D-6	8.05	14420	58.73	59.31	28.58
D-7	8.45	11800	54.74	55.58	26.64

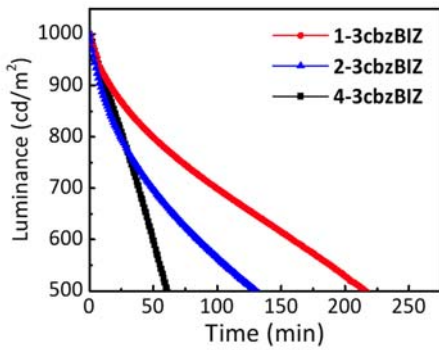


Fig. S23 Luminance decay curves for **1**-, **2**- and **4-3cbzBIZ** in blue OLEDs at initial luminance of $1000 \text{ cd}/\text{m}^2$.

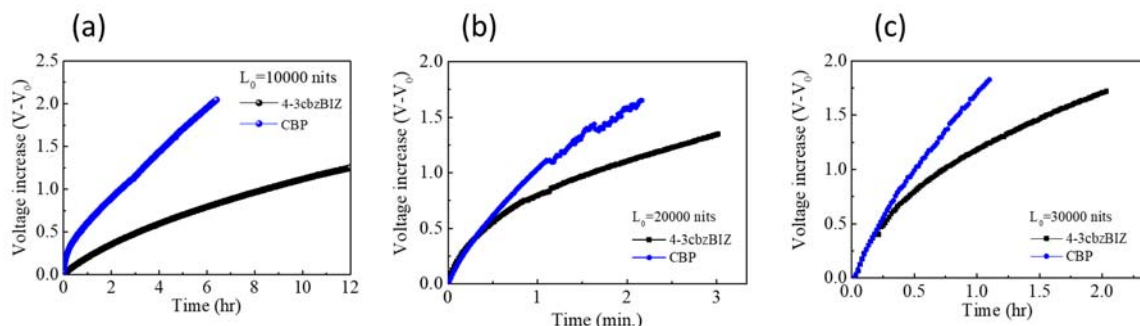


Fig. S24 Driving voltage changes with aging time for initial luminescence of (a) 10000; (b) 20000; (c) 30000 cd/m^2

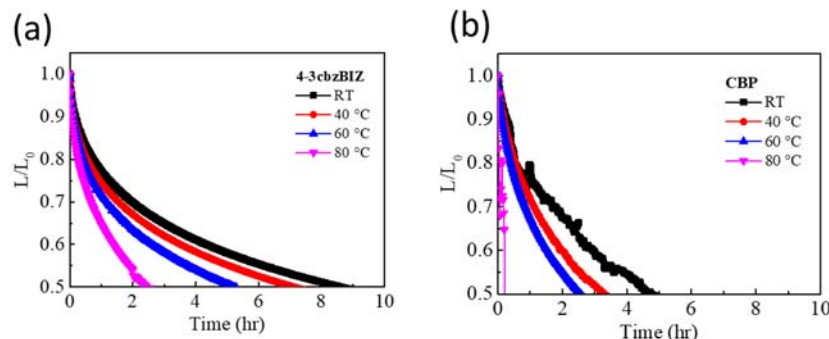


Fig. S25 Luminance decay curves of (a) **4-3cbzBIZ** and (b) CBP devices under different temperature at initial luminance of $10000 \text{ cd}/\text{m}^2$.

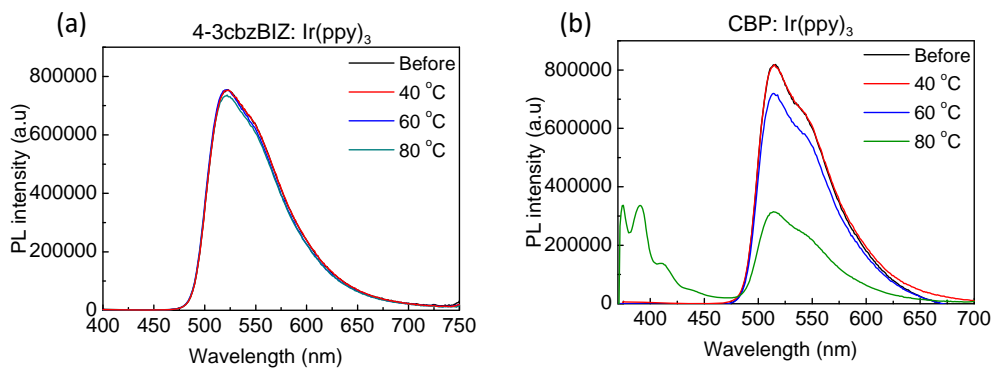


Figure S26 PL spectra of doped films of (a) **4-3cbzBIZ:10%Ir(ppy)₃** and (b) **CBP: 10%Ir(ppy)₃** before and after with annealing of 40 °C, 60 °C, 80 °C for 30 mins.

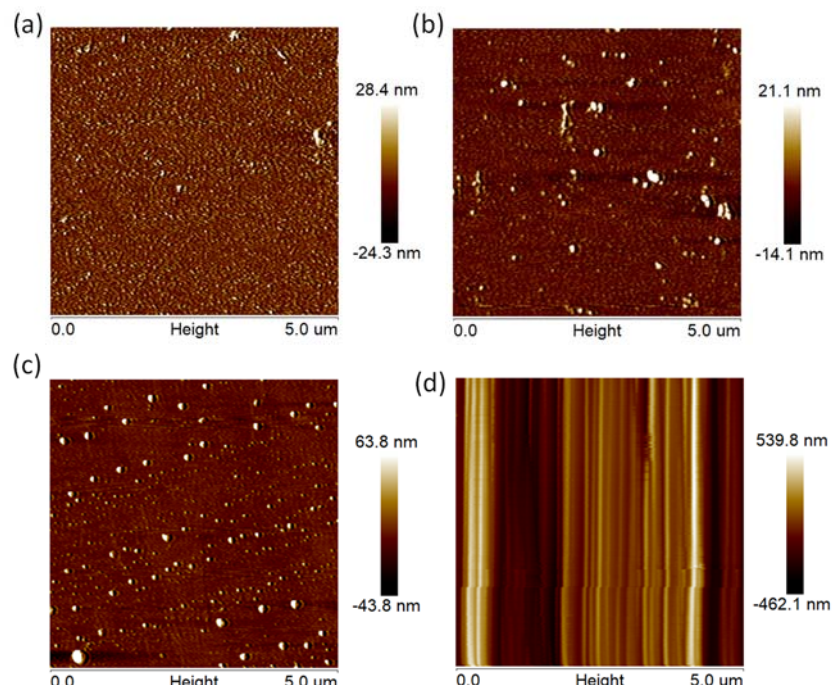


Figure S27 AFM images of doped films before and after annealing at a high temperature (80 °C) of **4-3cbzBIZ:10%Ir(ppy)₃** (a) before (b) after, and **CBP: 10%Ir(ppy)₃** (c) before (d) after, respectively.